

AD-A227 655

DTIC FILE COPY

1

1990

Thesis/Dissertation

An Investigation of a Gravity Wave During GALE:
6 February 1986

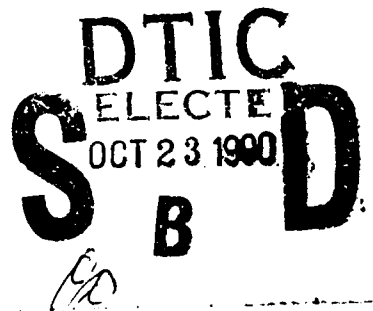
Kenneth S. Smith

AFIT Student at: North Carolina State University

AFIT/CI/CIA -90-078

AFIT/CI
Wright-Patterson AFB OH 45433

Approved for Public Release IAW AFR 190-1
Distribution Unlimited
ERNEST A. HAYGOOD, 1st Lt, USAF
Executive Officer, Civilian Institution Programs



GENERAL INSTRUCTIONS FOR COMPLETING SF 298

The Report Documentation Page (RDP) is used in announcing and cataloging reports. It is important that this information be consistent with the rest of the report, particularly the cover and title page. Instructions for filling in each block of the form follow. It is important to **stay within the lines to meet optical scanning requirements.**

Block 1. Agency Use Only (Leave Blank)

Block 2. Report Date. Full publication date including day, month, and year, if available (e.g. 1 Jan 88). Must cite at least the year.

Block 3. Type of Report and Dates Covered. State whether report is interim, final, etc. If applicable, enter inclusive report dates (e.g. 10 Jun 87 - 30 Jun 88).

Block 4. Title and Subtitle. A title is taken from the part of the report that provides the most meaningful and complete information. When a report is prepared in more than one volume, repeat the primary title, add volume number, and include subtitle for the specific volume. On classified documents enter the title classification in parentheses.

Block 5. Funding Numbers. To include contract and grant numbers; may include program element number(s), project number(s), task number(s), and work unit number(s). Use the following labels:

C - Contract	PR - Project
G - Grant	TA - Task
PE - Program Element	WU - Work Unit Accession No.

Block 6. Author(s). Name(s) of person(s) responsible for writing the report, performing the research, or credited with the content of the report. If editor or compiler, this should follow the name(s).

Block 7. Performing Organization Name(s) and Address(es). Self-explanatory.

Block 8. Performing Organization Report Number. Enter the unique alphanumeric report number(s) assigned by the organization performing the report.

Block 9. Sponsoring/Monitoring Agency Name(s) and Address(es). Self-explanatory.

Block 10. Sponsoring/Monitoring Agency Report Number. (If known)

Block 11. Supplementary Notes. Enter information not included elsewhere such as: Prepared in cooperation with...; Trans. of ..., To be published in When a report is revised, include a statement whether the new report supersedes or supplements the older report.

Block 12a. Distribution/Availability Statement.

Denote public availability or limitation. Cite any availability to the public. Enter additional limitations or special markings in all capitals (e.g. NOFORN, REL, ITAR)

DOD - See DoDD 5230.24, "Distribution Statements on Technical Documents."

DOE - See authorities

NASA - See Handbook NHB 2200.2.

NTIS - Leave blank.

Block 12b. Distribution Code.

DOD - DOD - Leave blank

DOE - DOE - Enter DOE distribution categories from the Standard Distribution for Unclassified Scientific and Technical Reports

NASA - NASA - Leave blank

NTIS - NTIS - Leave blank.

Block 13. Abstract. Include a brief (Maximum 200 words) factual summary of the most significant information contained in the report.

Block 14. Subject Terms. Keywords or phrases identifying major subjects in the report.

Block 15. Number of Pages. Enter the total number of pages.

Block 16. Price Code. Enter appropriate price code (NTIS only).

Blocks 17. - 19. Security Classifications.

Self-explanatory. Enter U.S. Security Classification in accordance with U.S. Security Regulations (i.e., UNCLASSIFIED). If form contains classified information, stamp classification on the top and bottom of the page.

Block 20. Limitation of Abstract. This block must be completed to assign a limitation to the abstract. Enter either UL (unlimited) or SAR (same as report). An entry in this block is necessary if the abstract is to be limited. If blank, the abstract is assumed to be unlimited.

**An Investigation of a Gravity Wave
During GALE: 6 February 1986**

By

Captain Kenneth S. Smith, USAF

A thesis in partial fulfillment of the Master of Science degree at North Carolina State University,
Raleigh N.C. 1990. 60 pp.

ABSTRACT

SMITH, KENNETH S. An Investigation of a Gravity Wave during GALE: 6 February 1986 (Under the direction of Gerald F. Watson and Steven Businger.)

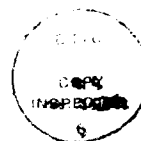
A mesoscale inertia-gravity wave that propagated northeastward across the southeastern United States on 6 February 1986 is investigated. Barograph traces and surface pressure perturbations based on hourly observations were used to trace the wave to its origin in the northwest Gulf of Mexico. The analysis shows that the wave propagated in the direction of the mid- and upper-tropospheric flow for over 19 hours at a mean speed of 25 ms^{-1} . The wave initially expanded as an arc, but the northern edge became bounded by a frontal system. Over the entire event, the half-period ranged from 25 minutes near its origin to 2 hours at the U.S. east coast. The half-wavelength is about 130 km with a crest to trough pressure range of less than 1.0 up to 5.7 mb along the axis of propagation.

Potential source mechanisms for the gravity wave were examined. These included orographic forcing; shear instability; geostrophic adjustment; density impulses and convection. Available evidence leads to the conclusion that intense and explosively growing convection provided the initial energy. After its initiation the gravity wave marked the sharp western edge of a convective line moving eastward along the Gulf Coast.

The long-lived horizontal propagation of the gravity wave is shown to be the result of a ducting structure within the mean flow. This structure was revealed by Richardson number and critical level profiles at several sounding stations along the wave path. The duct is eventually disrupted by the frontal structure which marks the northern edge of the gravity wave.

Forecasting the formation of a large amplitude gravity wave is still a challenge although the general synoptic context seems common among several gravity wave cases

(Uccellini and Koch, 1987). However, once such a wave is detected, forecasters along the wave path should be alerted to significant weather events that often accompany such phenomena.



Accession For	
NTIS GRA&I	<input checked="checked" type="checkbox"/>
DTIC TAB	<input type="checkbox"/>
Unannounced	<input type="checkbox"/>
Justification	
By	
Distribution/	
Availability Codes	
Dist	Avail and/or Special
A-1	

BIBLIOGRAPHY

- Atkinson, B.W., 1981: Mesoscale Atmospheric Circulations. Academic Press.,pp 283-309.
- Balachandran, N.K.,1980: Gravity Waves from Thunderstorms. *Mon. Wea. Rev.*, **108**, 804-816.
- Barnes, S. L., 1964: A Technique for maximizing details in numerical weather map analysis. *J. Appl. Meteor.*, **3**, 396-409.
- ,1973: Mesoscale objective map analysis using weighted time series observations. NOAA Technical Memorandum ERL NSSL-62, Norman, Ok,60pp.
- , 1985: Omega diagnostics as a supplement to LFM/MOS guidance in weakly forced convective situations. *Mon. Wea. Rev.*, **113**, 2122-2141.
- Bluestein, H.B., 1986: Fronts and Jet Streaks: A theoretical perspective. Mesoscale Meteorology and Forecasting. American Meteorological Society, 793 pp.
- Booker, J. R. and F.P. Bretherton, 1967: The critical layer for internal gravity waves in a shear flow. *J. Fluid Mech.*, **27**, 513-559.
- Bosart, L. F. and A. Seimon, 1988: A case study of an unusually intense gravity wave. *Mon. Wea. Rev.*, **116**, 1857-1886.
- Brunk, I.W., 1949: The pressure pulsation of April 11,1944. *J. Meteor.*, **6**, 395-401.
- Byers, H.R., 1974: General Meteorology. McGraw-Hill, Inc., New York, 236 pp.
- DeMaria, M., J.M. Davis, and D.M. Wojtak, 1989: Observations of mesoscale wave disturbances during the Genesis of Atlantic Lows Experiment. *Mon. Wea. Rev.*, **117**, 826-842.

Dirks, R. A., J.P. Kuettner and J.A. Moore, 1988: Genesis of Atlantic Lows Experiment (GALE): An overview. *Bull. Amer. Meteor. Soc.*, **69**, 148-160.

Erickson, C.O., and L.F. Whitney, Jr., 1973: Gravity waves following severe thunderstorms. *Mon. Wea. Rev.*, **101**, 708-711.

Gear, J. A., and R. Grimshaw, 1983: A second-order theory for solitary waves in shallow fluid. *Phys. Fluid*, **26**, 14-29.

Gedzelman, S.D., 1983: Short-period atmospheric gravity waves: A study of their statistical properties and source mechanisms. *Mon. Wea. Rev.*, **111**, 1293-1299.

-----, and R.A. Rilling, 1978: Short-period atmospheric gravity waves: A study of their dynamic and synoptic features. *Mon. Wea. Rev.*, **106**, 196-210.

Gossard, E.E., and W. Munk, 1954: On gravity waves in the Atmosphere. *J. of Meteor.*, **11**, 259-269.

-----, and W.H. Hooke, 1975: Waves in the Atmosphere. Developments in atmospheric science, II. Elsevier Scientific Publishing Co., Amsterdam, 456 pp.

Hoskins, B.J., I. Draghici, and H.C. Davies, 1978: A new look at the omega -equation. *Quart. J. Roy. Meteor. Soc.*, **104**, 31-38.

Hooke, W.H., 1984: Gravity Waves. AMS intensive course on mesoscale Meteorology and Forecasting, AMS, Boston, Mass. 345 pp.

Kaplan, M.L., and D.A. Paine, 1977: The observed divergence of the horizontal velocity field and pressure gradient force at the mesoscale: Its implications for the parameterization of three-dimensional momentum transport in synoptic-scale numerical models. *Beitr. Phys. Atmos.*, **50**, 321-330.

Koch, S.E., 1979: Mesoscale gravity waves as a possible trigger of severe convection along a dryline. Ph.D. Thesis, University of Oklahoma, 195 pp.

Kreitzberg, C.W., and T.J. Mercer, 1986: Genesis of Atlantic Lows Experiment (GALE) Field Program Summary. Drexel University, Philadelphia, Pa., 217 pp.

Lin, Y.-L., and R.C. Goff, 1988: A study of a mesoscale solitary wave in the atmosphere originating near a region of deep convection. *J. Atmos. Sci.*, **45**, 194-204.

Lindzen, R.S., 1974: Wave-CISK in the tropics. *J. Atmos. Sci.*, **31**, 156-179

-----, and K.-K. Tung, 1976: Banded convective activity and ducted gravity waves. *Mon. Wea. Rev.*, **104**, 1602-1617.

Moore, J. T. and P. D. Blakley, 1988: The role of frontogenetical forcing and conditional instability in the midwest snowstorm of 30-31 January 1982. *Mon. Wea. Rev.*, **116**, 2155-2171.

O'Brien, J.J., 1970: Alternative solutions to the classical vertical velocity problem. *J. Appl. Meteor.*, **9**, 197-203.

Pencik, M.J., and J.A. Young, 1984: Mechanics of a strong sub-synoptic gravity wave deduced from satellite and surface observations. *J. Atmos. Sci.*, **41**, 1850-1862.

Raymond, D.J., 1975: A model for predicting the movement of continuously propagating convective storms. *J. Atmos. Sci.*, **32**, 1308-1317.

Rawlings, J.O., 1988: Applied Regression Analysis: a research tool. Wadsworth and Brooks/ Cole Advanced books and Software, 553 pp.

Shapiro, R., 1975: Linear Filtering. *Math. Comp.*, **29**, 1094-1097.

Smith, R.B., and Y.-L. Lin, 1982: The addition of heat to a stratified airstream with application to the dynamics of orographic rain. *Quart. J. Roy. Meteor. Soc.*, **108**, 353-378.

Tepper, M., 1950: A proposed mechanism of squall lines: The pressure jump line. *J. Meteor.*, **7**, 21-29.

Uccellini, L.W., 1975: A case study of apparent gravity wave initiation of severe convective storms. *Mon. Wea. Rev.*, **103**, 497-513.

-----, and S.E. Koch, 1986: The synoptic setting and possible energy sources for mesoscale wave disturbances. *Mon. Wea. Rev.*, **115**, 721-729.

Van Tuyl, A.H., and J.A. Young, 1982: Numerical simulation of nonlinear jet streak adjustment. *Mon. Wea. Rev.*, **110**, 2038-2054.

Wojtak, D.M., 1987: Observation of gravity waves during the Genesis of Atlantic Lows Experiment. M.S. Thesis, North Carolina State University, 75 pp.

An Investigation of a Gravity Wave

During GALE: 6 February 1986

by

Kenneth Steven Smith

A thesis submitted to the Graduate Faculty of
North Carolina State University
in partial fulfillment of the requirements for the Degree of
Master of Science

Department of Marine, Earth & Atmospheric Sciences

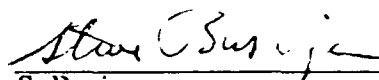
Raleigh

1990

Approved by:


G. F. Watson

Co-Chairman of Advisory Committee


S. Businger

Co-Chairman of Advisory Committee


D. W. Nychka

ABSTRACT

SMITH, KENNETH S. An Investigation of a Gravity Wave during GALE: 6 February 1986 (Under the direction of Gerald F. Watson and Steven Businger.)

A mesoscale inertia-gravity wave that propagated northeastward across the southeastern United States on 6 February 1986 is investigated. Barograph traces and surface pressure perturbations based on hourly observations were used to trace the wave to its origin in the northwest Gulf of Mexico. The analysis shows that the wave propagated in the direction of the mid- and upper-tropospheric flow for over 19 hours at a mean speed of 25 ms^{-1} . The wave initially expanded as an arc, but the northern edge became bounded by a frontal system. Over the entire event, the half-period ranged from 25 minutes near its origin to 2 hours at the U.S. east coast. The half-wavelength is about 130 km with a crest to trough pressure range of less than 1.0 up to 5.7 mb along the axis of propagation.

Potential source mechanisms for the gravity wave were examined. These included orographic forcing; shear instability; geostrophic adjustment; density impulses and convection. Available evidence leads to the conclusion that intense and explosively growing convection provided the initial energy. After its initiation the gravity wave marked the sharp western edge of a convective line moving eastward along the Gulf Coast.

The long-lived horizontal propagation of the gravity wave is shown to be the result of a ducting structure within the mean flow. This structure was revealed by Richardson number and critical level profiles at several sounding stations along the wave path. The duct is eventually disrupted by the frontal structure which marks the northern edge of the gravity wave.

Forecasting the formation of a large amplitude gravity wave is still a challenge although the general synoptic context seems common among several gravity wave cases

(Uccellini and Koch, 1987). However, once such a wave is detected, forecasters along the wave path should be alerted to significant weather events that often accompany such phenomena.

Acknowledgments

It is the author's distinct pleasure to thank those who made this thesis possible. At the risk of making an embarrassing omission, I would like to extend a special "Thank-you" to the following:

My fellow classmates; whose help, insights and encouragement were invaluable. In particular I want to thank Capt Bud Zinni, Ron Weglarz, Steve Chiswell, Capt Laureleen O'Connor and Capt Ron Dunic.

Dr.'s Yuh-Lang Lin and Mark DeMaria for their advice and support.

Special thanks and love go to my wife Barbara and my two daughters - Danielle and Amanda. They mean everything.

Table of Contents

	Page
LIST OF TABLES	iv
LIST OF FIGURES	v
LIST OF SYMBOLS AND ABBREVIATIONS	ix
1. INTRODUCTION	1
2. HISTORY OF WAVE PROPAGATION	9
2.1 Synoptic Setting	9
2.2 Determining the Location of Wave Origin	12
3. WAVE LONGEVITY	24
3.1 Atmospheric Ducting	24
3.2 Vertical Atmospheric Structure	25
4. WAVE INITIATION	34
4.1 Orographic Forcing	34
4.2 Shear Instability	34
4.3 Geostrophic Adjustment	36
4.4 Density Impulses	37
4.5 Convection	41
5. DISCUSSION AND CONCLUSIONS	51
6. LIST OF REFERENCES	55
7. APPENDIX - Objective Analysis Scheme and Numerical Calculations	59

LIST OF TABLES

	Page
6.1 Correlation Matrix.....	53

LIST OF FIGURES

	Page
1.1 PAM II Data (a) perturbation pressure; (b) filtered winds; (c) filtered horizontal divergence; (d) hourly rainfall. All are for case 4, 6 February 1986 at 1900 UTC (From DeMaria et al, 1989).....	2
1.2 A schematic representation of the surface wave structure (From DeMaria et al, 1989).....	3
1.3 Flight track of NCAR Electra aircraft from 1847 - 1956 UTC 6 February 1986. Arrows show the direction of flight. Aircraft intersection with the gravity wave was at an altitude of 10,000 feet.....	5
1.4 (a) Temperature and Dew Point ($^{\circ}$ C) as measured during NCAR Electra flight 1910 - 1940 UTC 6 February 1986. (b) Wind direction (degrees) and speed (ms^{-1}) during same aircraft flight as in (a).....	6
2.1 (a) Surface analysis with sea level pressure (solid lines) at 0000 UTC 6 February 1986. Dashed lines are isotherms ($^{\circ}$ F).....	10
2.1 (b) 500 mb analysis at 0000 UTC 6 February 1986. Height contours (solid lines) in decameters. Dashed lines are absolute vorticity (10^{-5} S^{-1}).....	11
2.1 (c) 300 mb analysis at 0000 UTC 6 February 1986. Solid lines are height contours (decameters). Dashed lines are isotachs (ms^{-1}).....	13
2.2 Barogram for Columbia, SC from 5 February 1986 1300 LST until 7 February 0430 LST. Note sharp pressure fall ~ 6 February 1330 LST.....	14
2.3 Altimeter settings from 1200 UTC until 2400 UTC 6 February. Wave passage at Macon, GA (MCN) ~ 1500 UTC; Augusta, GA (AGS) ~ 1830 UTC; Columbia, SC (CAE) ~ 1830 UTC and Florence, SC (FLO) ~ 2100 UTC.....	15

2.4	Wave propagation. Thin solid lines are isochrones of pressure trough (time in UTC shown at bottom). Individual reporting stations located at the dots show the reported pressure perturbation with wave passage. These values (mb) are isoplethed by the dashed lines. The locus of maximum perturbations is shown by the arrow. The heavy solid line is the local position of frontal boundaries with respect to the isochrone times.....	16
2.5	(a) Radar summary 0935 UTC 6 February 1986. (b) 1335 UTC 6 February.....	18
2.5	(c) Radar summary 1735 UTC 6 February 1986. (d) 2135 UTC 6 February.....	19
2.5	(e) Radar summary 0135 UTC 7 February 1986.....	20
2.6	(a) Digitized radar summary from Slidell, LA 0727 UTC 6 February 1986. Numbers 1-9 indicate precipitation intensity levels, with 9 being "unknown". (b) Same as (a) except 0425 UTC 6 February.....	21
2.7	Radar summary 0135 UTC 6 February 1986. Backtrack timeline from Slidell, LA is shown.....	22
2.8	Geostationary Operational Environmental Satellite (GOES) infrared imagery at 0130 UTC 6 February 1986.....	23
3.1	(a) Richardson number (Ri) and Brunt-Vaisala frequency (N) vertical profiles for Boothville, LA 0000 UTC 6 February 1986. (b) Same as (a) except for Apalachicola, FL 1200 UTC 6 February.....	26
3.2	Same as figure 3.1 except for (a) Centerville, AL (b) Waycross, GA 1200 UTC 6 February 1986. (c) Asheville, NC 1800 UTC and (d) Beaufort, NC 2100 UTC 6 February.....	28
3.3	Same as figure 3.1 except for Athens, GA 1200 UTC 6 February 1986.....	29

3.4	Position of "back-door" cold front at 3-hour intervals from 1800 UTC 6 February 1986 until 0000 UTC 7 February 1986.....	31
3.5	Barogram from Elizabeth City, NC. Time scale of trace is from 5 February 1300 LST until 7 February 1530 LST. Note gravity wave signature on 6 February from 1700-1900 LST.....	32
3.6	Same as figure 3.1 except for Petersburg, VA 0000 UTC 7 February 1986.....	33
4.1	Wave amplitudes as a function of minimum Richardson number in the sounding. The envelope indicates that large-amplitude waves are not expected from shear instability. (After Gedzelman and Rilling, 1978).....	35
4.2	The ageostrophic motions (arrows) and associated convergence (CON) and divergence (DIV) patterns in the vicinity of a jet streak. (From Bluestein, 1986).....	38
4.3	(a) 600 mb vertical velocity (10^{-5} S^{-1}) at 12 hours into three numerical models. Mean flow is left to right. Jet core location at 400 mb is marked with an X. (b) Divergence field for experiment in (a). (c) same as (b) (From Van Tuyl and Young, 1982).....	39
4.4	Horizontal divergence (10^{-6} S^{-1}) at 300 mb 0000 UTC 6 February 1986. Jet streak location indicated by the arrow.....	40
4.5	Position of frontal system at 3-hour intervals from 5 February 1800 UTC until 6 February 0600 UTC.....	42
4.6	Gravity-wave generation by penetrative convection. (From Hooke, 1984).....	43
4.7	(a) Radar summary 1735 UTC 5 February 1986. (b) Same as in (a) except for 1935 UTC 5 February.....	44
4.8	Same as Figure 2.8 except visible imagery at 1930 UTC 5 February 1986.....	45

4.9 Same as Figure 2.8 except at 2000 UTC 5 February 1986.....	46
4.10 Same as Figure 2.8 except at 2200 UTC 5 February 1986.....	47
4.11 Same as Figure 2.8 except at 0230 UTC 6 February 1986.....	48
4.12 Skew-T Log-P diagram for Boothville, LA at 0000 UTC 6 February 1986. Temperature and dew point are indicated by the bold solid and dashed lines respectively.....	50

List of Symbols and Abbreviations

$^{\circ}\text{C}$	Degrees Centigrade
C	Phase speed of wave frequency
C_d	Phase speed in a duct
C_L	Critical level
CON	Convergence
d^2	Grid distance squared
Dew pt	Dew point temperature
DIV	Divergence
exp	Exponential
$^{\circ}\text{F}$	Degrees Fahrenheit
g	Gravitational constant ($\sim 9.8 \text{ ms}^{-2}$)
GALE	Genesis of Atlantic Lows Experiment
GOES	Geostationary Operational Environmental Satellite
H	Depth of duct
k_0	Weight parameter
km	Kilometers
LST	Local Standard Time
mb	Millibars
mph	Miles per hour
ms^{-1}	Meters per second
n	Wave mode number
N	Brunt-Vaisala frequency
NCAR	National Corporation for Atmospheric Research
NWS	National Weather Service
PAM II	Second-generation Portable Automated Mesonet
Q	Mean of any meteorological variable
Q_i	Observed value of any meteorological variable at a grid point
R_i	Richardson number
R^{**2}	R-Square; square of the multiple correlation coefficient
S^{-1}	Per second
Temp	Temperature
u	Velocity component in X-direction

U_0	Mean horizontal velocity
w_i	Observational weight given to a meteorological variable
Wind Dir	Wind direction
z	Vertical axis
Δ	Change notation
Σ	Sum of
$>$	Greater than
$<$	Less than
π	Pi, the constant (~ 3.14)
μbar	Microbars

1. Introduction

On 6 February 1986 a mesoscale wave propagated east-northeastwards from the Gulf of Mexico across the southeastern United States. This mesoscale feature (horizontal wavelength approximately 250 km) was unusual in the sense that it was long-lived (over 19 hours) and had a dramatic effect on the sensible weather over a large geographical area. As a type of solitary gravity wave, this event is not unique. Propagating gravity waves of this scale are often observed in the atmosphere (Lin and Goff, 1988). Some have been known to initiate or enhance strong convection (Uccellini, 1975) while others seem to be the predominant cause of clear air turbulence (Hooke, 1984). More fundamentally, gravity waves are thought to be a major process in the atmospheric exchange of energy from larger to smaller scales of motion (Hooke, 1984).

During the period 4 to 6 February 1986, several mesoscale gravity-wave like disturbances moved through the Genesis of Atlantic Lows (GALE) experimental area. Resolution of these mesoscale features was feasible due to an array of 50 Portable Automated Mesonet (PAM II) stations in place across eastern North and South Carolina and southeast Virginia. The PAM II stations were spaced about 68 km apart and provided 5-minute averaged values of surface pressure at 5-minute intervals. Using filtered pressure data from these stations, DeMaria et al. (1989) were able to identify and document the basic horizontal and vertical structure of four distinct waves during the 4 to 6 February period.

Only one of the four waves identified maintained a constant wave structure as it moved through the PAM II network. It was the only wave that had a precipitation field moving with it, and also had the largest pressure perturbation ($\sim \pm 2$ mb). Wave parameters calculated by DeMaria et al during the 8 hour period (1600-2400 UTC 6 Feb) in which this wave propagated eastward through the PAM II network showed a phase speed of $20\text{--}30\text{ ms}^{-1}$, a half wavelength of 100-150 km, a period of 2-4 hours and a trough to crest pressure range of 2.0-3.5 mb. These numbers produce a Rossby number of approximately 1 and indicate an inertia-gravity wave.

Figure 1.1 shows the two-dimensional structure of the wave at 1900 UTC on 6 February. The same calculations were accomplished for this case at other times (not shown) and led to a simple conceptual model of the horizontal and vertical structure of a solitary wave of depression. Figure 1.2 (from DeMaria et al, 1989) summarizes this concept. Note that precipitation ends just prior to the passage of surface divergence which precedes the pressure minimum.

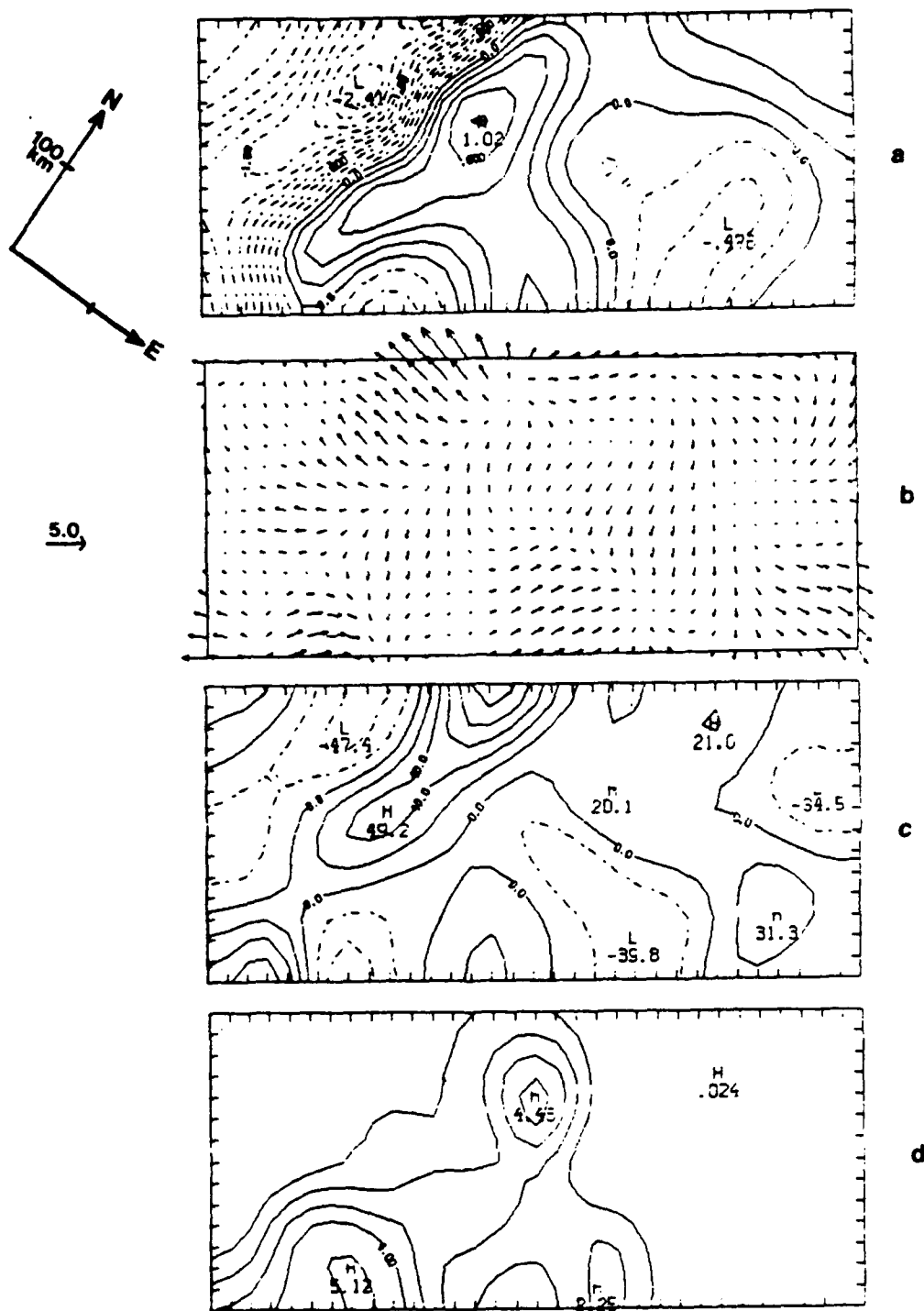


Figure 1.1 PAM II Data (a) perturbation pressure; (b) filtered winds; (c) filtered horizontal divergence; (d) hourly rainfall. All are for case 4, 6 February 1986 at 1900 UTC (From DeMaria et al, 1989).

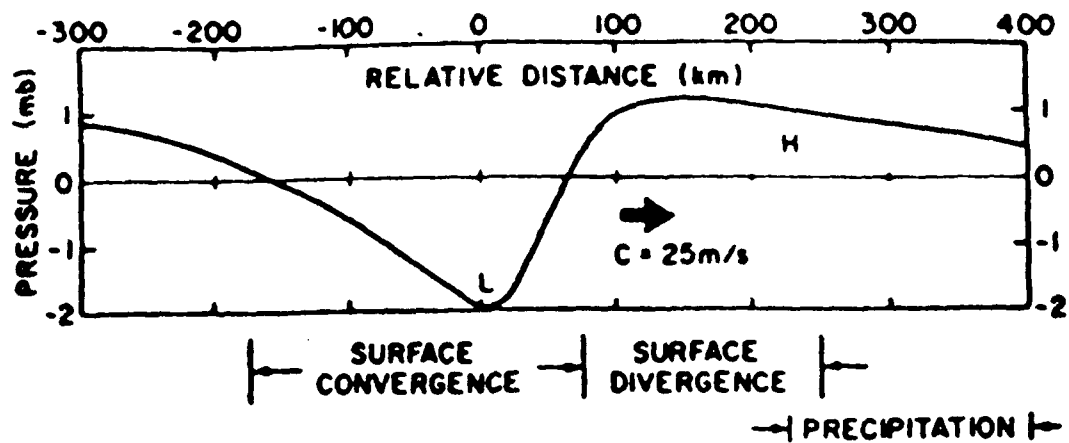


Figure 1.2 A schematic representation of the surface wave structure (From DeMaria et al, 1989).

Although figure 1.2 shows surface convergence west of the pressure minimum, the atmosphere was much too dry for precipitation in this region. Data from the NCAR Electra flight on 6 February supports this. Figure 1.3 shows the flight path. Of particular note here is the flight loop in South Carolina which transected the wave as the latter approached the coast.

From the mission summary (Kreitzberg and Mercer, 1986): "... Dry air moved across CAE (Columbia, S.C.) to the coast by the final loop. An extremely sharp shear zone was encountered aloft between CHS (Charleston, S.C.) and CAE....". Figure 1.4 shows both the sudden change in the wind field and the rapid drying after saturated conditions as the Electra crossed the wave front at approximately 1920 UTC, .

Considerable research (both observational and theoretical) has been conducted in the past on the manifestation and nature of gravity waves. A linear analysis of the hydrodynamic set of equations has two solutions that describe gravity waves. Furthermore, many authors have investigated this wave phenomena using nonlinear theory (e.g., Gear and Grimshaw, 1983). However, it is the physical structure of these waves in the atmosphere which is the focus of this thesis.

An early observational study was done by Brunk in 1944. In that case, a "pressure pulsation" was observed to move eastward from Missouri to off the southern New England coast at a speed between 35 and 50 mph with pressure falls of 3-15 mb in a short period of time (< 3 hrs.). The event lasted for at least 24 hours with nearly all barograms studied along the wave path exhibiting a "V" type signature with the station pressure never recovering to pre-event levels (Brunk, 1949).

Brunk notes that the initiation was "probably the result of ... thunderstorm activity, although the largest pulsation occurred in an area where thunderstorms were not observed."

The pressure falls observed by Brunk are contrasted with Tepper's (1950) hypothesis of squall lines resulting from gravity waves moving along an inversion in the warm sector. In this case, a pressure "jump" of noticeable magnitude is associated with thunderstorm activity. Other gravity wave oscillations occurring in conjunction with temperature inversions have not been tied to convection. Gossard and Munk (1954) examine an event in Southern California where only fog and stratus accompany the wave.

It is apparent that gravity waves display differing characteristics in the atmosphere. They have been observed with a wide range of wavelengths, amplitudes and phase speeds (Wojtak, 1987). This is not surprising considering the different types of mechanisms that

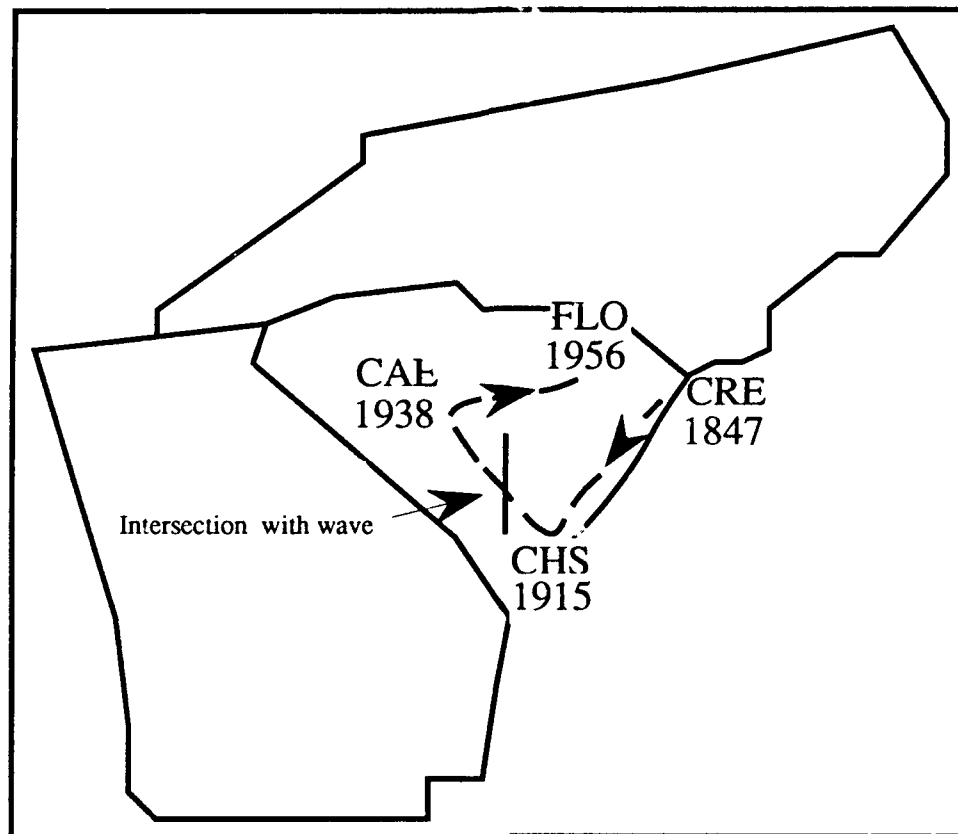


Figure 1.3 Flight track of NCAR Electra aircraft from 1847 - 1956 1986. Arrows show the direction of flight. Aircraft intersection with wave was at an altitude of 10,000 feet.

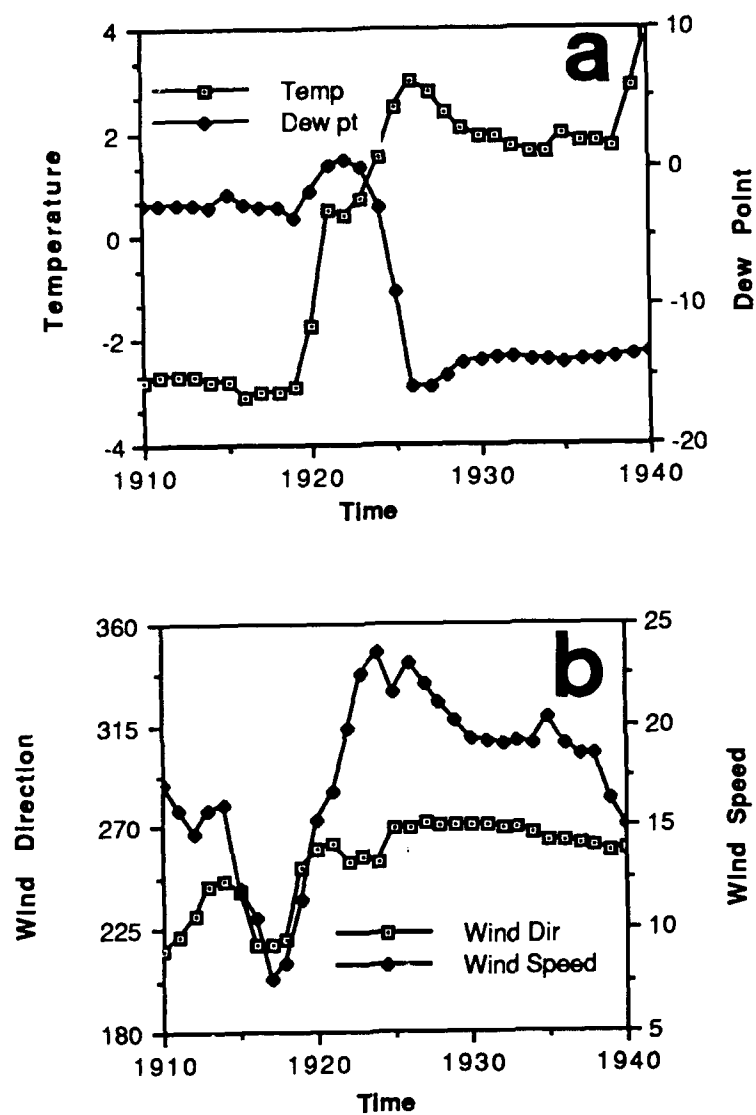


Figure 1.4 (a) Temperature and Dew Point ($^{\circ}$ C) as measured during NCAR Electra flight 1910 - 1940 UTC 6 February 1986. (b) Wind direction (degrees) and speed (ms^{-1}) during same aircraft flight as in (a).

can generate these waves: shear instability, density impulses, geostrophic adjustment, orographic and thermal forcing (Gossard & Hooke, 1975) being among them.

The amplitude of the wave's pressure perturbation is of importance in determining how the local weather is affected. It has been demonstrated (Koch, 1979) that ascent patterns associated with gravity waves can release the potential instability of surrounding air. This can trigger severe convection (Uccellini, 1975) with damaging surface winds. Even without convection, the perturbation's effect on the wind field can be dramatic. A 7 mb perturbation can cause a 15 m/s wind deviation (Pencik and Young, 1984). In the previously mentioned case of Brunk, wind gusts in excess of 20 m/s were common along the wave path. Hence, it would prove beneficial if the pressure amplitude could be predicted.

In regards to the longevity of gravity waves, it can be shown that if they were to propagate freely, they should not exist for more than one horizontal wavelength downstream. Gossard and Hooke (1975) show that for an incompressible, Boussinesq atmosphere, inertia-gravity waves can propagate their energy vertically through the troposphere very quickly. Therefore, to explain long duration events observed the waves must be either continuously created or somehow "trapped" by the vertical atmospheric structure.

Lindzen and Tung (1976) show that gravity waves may be ducted under certain conditions. The requirements are a statically stable propagation layer that is capped by a weakly stratified upper layer capable of reflecting the vertical wave energy. The wave energy is thus constrained to the layer bounded by the upper reflecting layer and (usually) the ground.

The objectives of the present research are to answer the following questions in relation to the GALE (Genesis of Atlantic Lows Experiment) gravity wave:

1. Where did the wave originate?
2. What was the physical mechanism that initiated the wave?
3. Why did the wave propagate over such a large horizontal distance?
4. What determined the observed ground speed of the wave?
5. What governed the amplitude of the pressure perturbation in time and space?

Can the amplitude be predicted?

In Chapter 2, the synoptic setting for this event is examined, and the wave is traced backward in time to its origin. After investigating the atmospheric structure for ducting mechanisms in Chapter 3, the probable initiating mechanism is identified in Chapter 4. In Chapter 5, statistical methods are used to postulate a method for predicting pressure perturbations given the fact that a mesoscale wave has been identified. Finally, the research is discussed and summarized in Chapter 6.

2. History of Wave Propagation

2.1 Synoptic Setting

On 5 February 1986 a long wave trough moved eastwards out of the southern Rocky Mountains into Texas, northern Mexico and the western Gulf of Mexico. A weak surface low pressure system with its associated frontal systems was drifting slowly east-northeastwards along the Texas Gulf coast. This low began to deepen after 1800 UTC with the approach of the upper level support.

At 1200 UTC 5 February 1986, the surface map (not shown) showed a wedge of cold air moving southwards from the Great Plains along the western slopes of the Rocky Mountains into northern and western Texas. A surface low pressure center was located in southeastern Texas with a cold front extending southwestwards into Mexico. A warm front on the northern side of this low quickly changes character to a cold front which then extends northeastwards towards Kentucky and Indiana.

The 500 mb height and vorticity analysis (not shown) for 1200 UTC 5 February showed a long wave trough extending southwards from Colorado into northern Mexico. The absolute vorticity is elongated north-south with the trough. A weak ridge is ahead of the trough over Texas in an otherwise southwesterly flow across the southeastern states.

The 300 mb chart at 1200 UTC 5 February (not shown) depicts a 45 ms^{-1} jet streak entering the base of the trough over the Gulf of California. Another band of strong winds (45 ms^{-1} plus) was located in the southwesterly flow from Texas northeastwards towards the lower Great Lakes.

By 0000 UTC 6 February, the surface analysis (fig 2.1a) shows colder air continuing to funnel southwards into Texas. The surface low pressure center is now located just offshore of Galveston, Texas. The low had filled from 5 February 0000 UTC until 1800 UTC, but then deepened 3 mb since 1800 UTC (map not shown). The associated cold front has pushed into the western Gulf while the northern extension of the front has become quasi-stationary as it lies parallel to the upper flow. Precipitation in the form of rain and rainshowers is occurring on the northern side of the low, while rather intense convection has developed east of the cold front and low over the Gulf.

The upper level trough axis at 500 mb has moved over Texas and become negatively tilted (Fig 2.1b). A vorticity maximum is located over southeastern Texas extending southeastwards into the Gulf of Mexico and northwestwards into New Mexico.

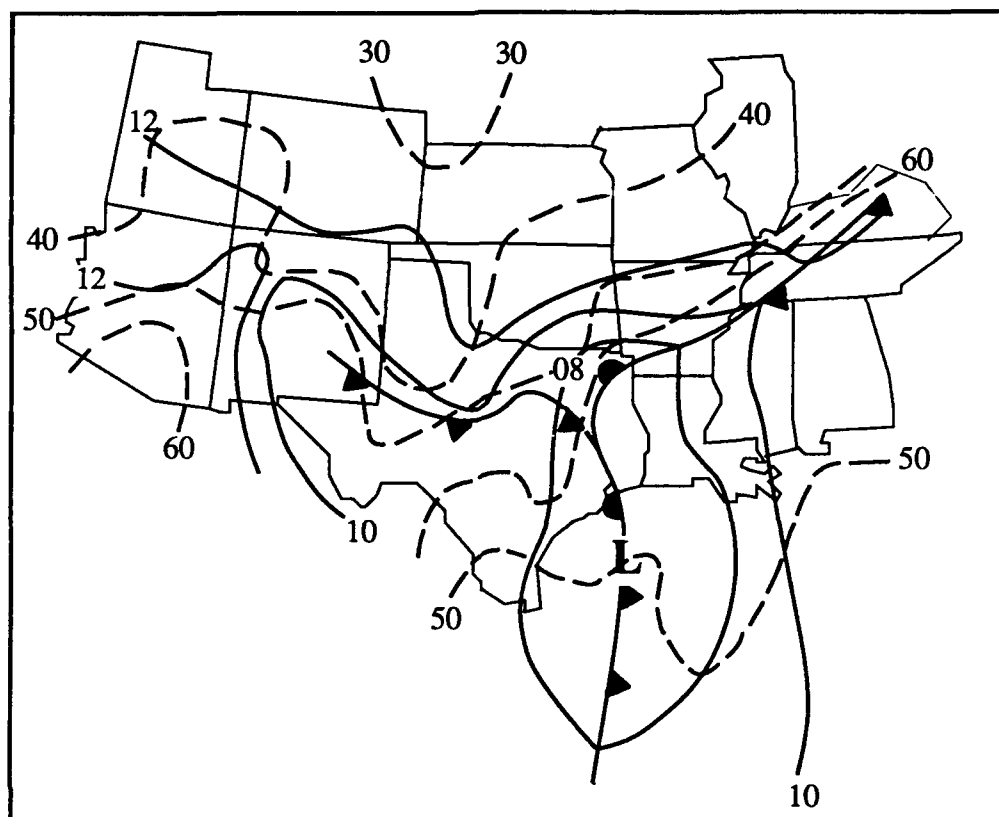


Figure 2.1 (a) Surface analysis with sea level pressure (solid lines) at 0000 UTC 6 February 1986. Dashed lines are isotherms ($^{\circ}$ F).

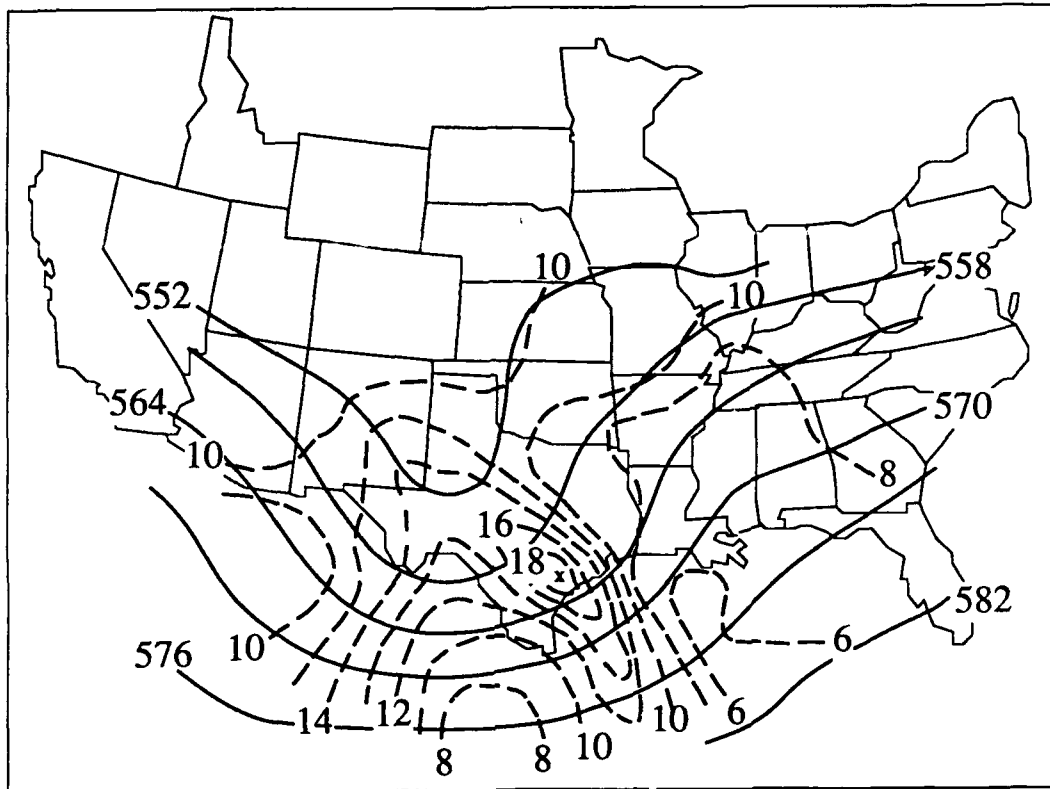


Figure 2.1 (b) 500 mb analysis at 0000 UTC 6 February 1986. Height contours (solid lines) in decameters. Dashed lines are absolute vorticity (10^{-5} s^{-1}).

The ridge just downstream has increased in amplitude with a vorticity minima located over the central Gulf and extending north-northwestwards.

At 300 mb on 6 February at 0000 UTC (fig 2.1c) the jet streak over the Gulf of California has moved around the base of the trough to a position along the Texas coast with winds exceeding 45 ms^{-1} .

2.2 Determining the Location of Wave Origin.

Since gravity waves are often identified by their signature in the surface pressure field (Atkinson, 1981), it was decided to trace the wave backward in time by examining pressure data across the southeastern states. To construct the most accurate isochrones possible, three distinct sets of data were used. First, all available barograph traces in the region were examined for evidence of a distinct, rapid pressure fall (for an example see fig. 2.2). Next, altimeter settings for over 80 stations were plotted at hourly intervals for evidence of the same phenomenon. As a practical matter, many more stations report altimeter setting than sea level pressure. Furthermore, altimeter setting is always reported in special observations - allowing a finer temporal resolution. Figure 2.3 shows the progression of the gravity wave from Georgia into South Carolina along with its associated steep pressure falls. The third data source was hourly surface pressure values available from the GALE data base. These data were filtered using a least squares technique to first remove the trend in order to examine pressure perturbations (Pencik and Young, 1984). Combining the results of all three data sets led to the analysis shown in fig. 2.4 between points A and B - isochrones of wave trough position and isopleths of wave amplitude.

The isochrones have been smoothed by hand as little as possible. Remaining undulations may be due more to errors associated with the pressure analysis than actual changes in the wave speed. This will be explained further in Chapter 3.

Of special interest at this juncture is the basic characteristics of the wave. The distance between points A and B in fig. 2.4 is 1370 km. The wave took 18 hours to cover this distance, resulting in a mean speed of about 21 m/s . Points A and B were chosen since they lie on the locus of maximum pressure perturbation, which is pointing to the northeast at an angle of about 60 degrees. This is in the direction of the mid- and upper tropospheric flow.

Note that the perturbations range from less than 1.0 to 5.7 mb. The actual barograph traces along the wave track show the half-period of the wave ranging from 25

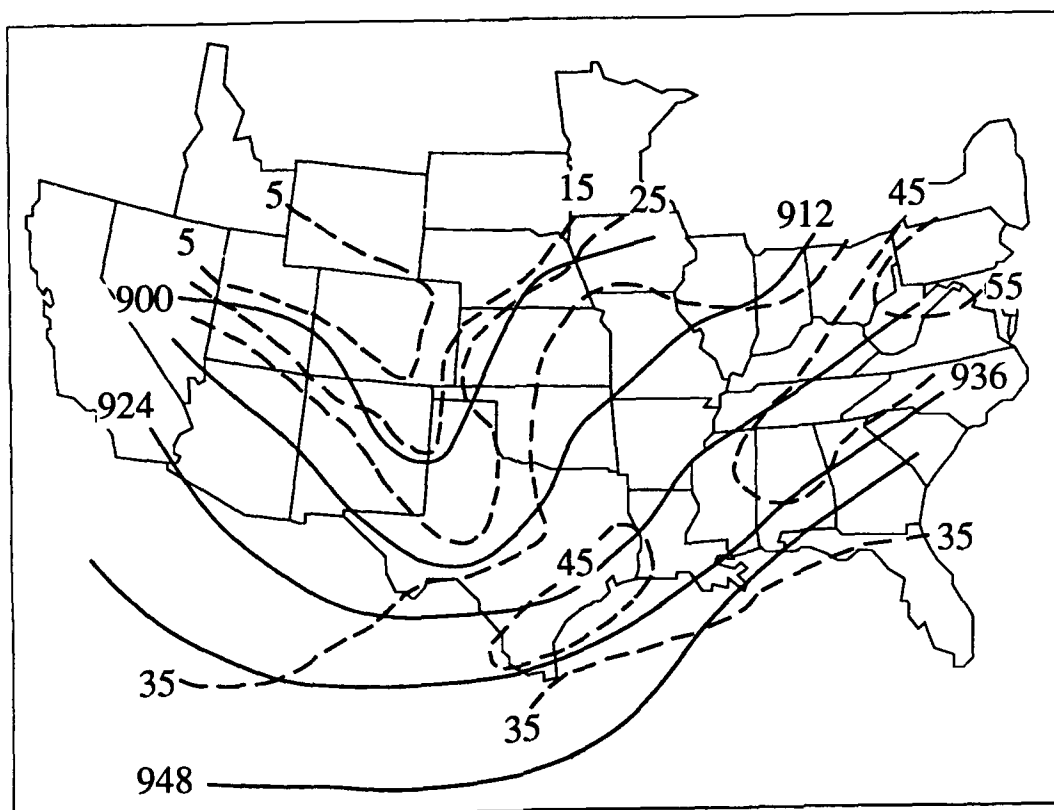


Figure 2.1 (c) 300 mb analysis at 0000 UTC 6 February 1986. Solid lines are height contours (decameters). Dashed lines are isotachs (ms^{-1}).

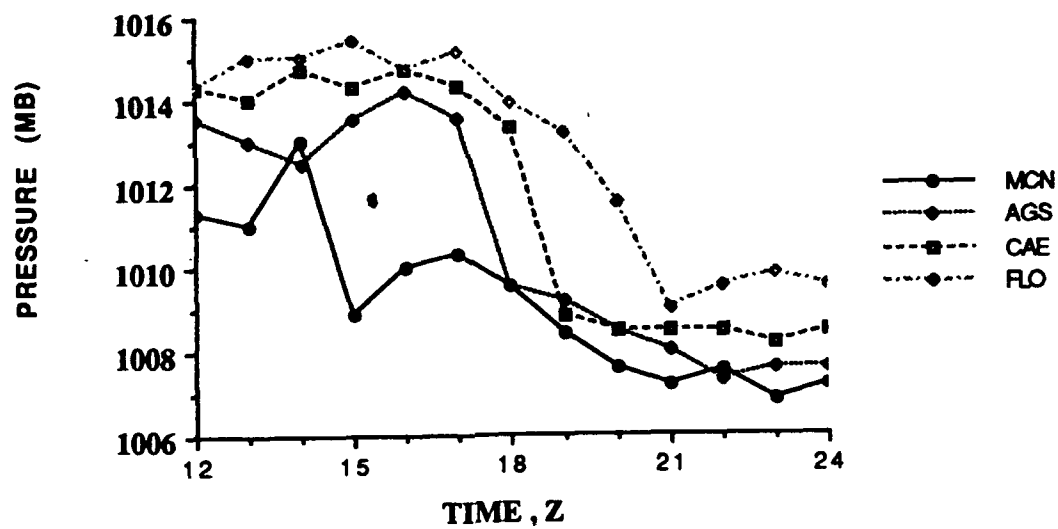


Figure 2.3 Altimeter settings from 1200 UTC until 2400 UTC 6 February at Macon, GA (MCN) ~ 1500 UTC; Augusta, GA (AGS) ~ 1830 UTC (CAE) ~ 1830 UTC and Florence, SC (FLO) ~ 2100 UTC.

sage
C

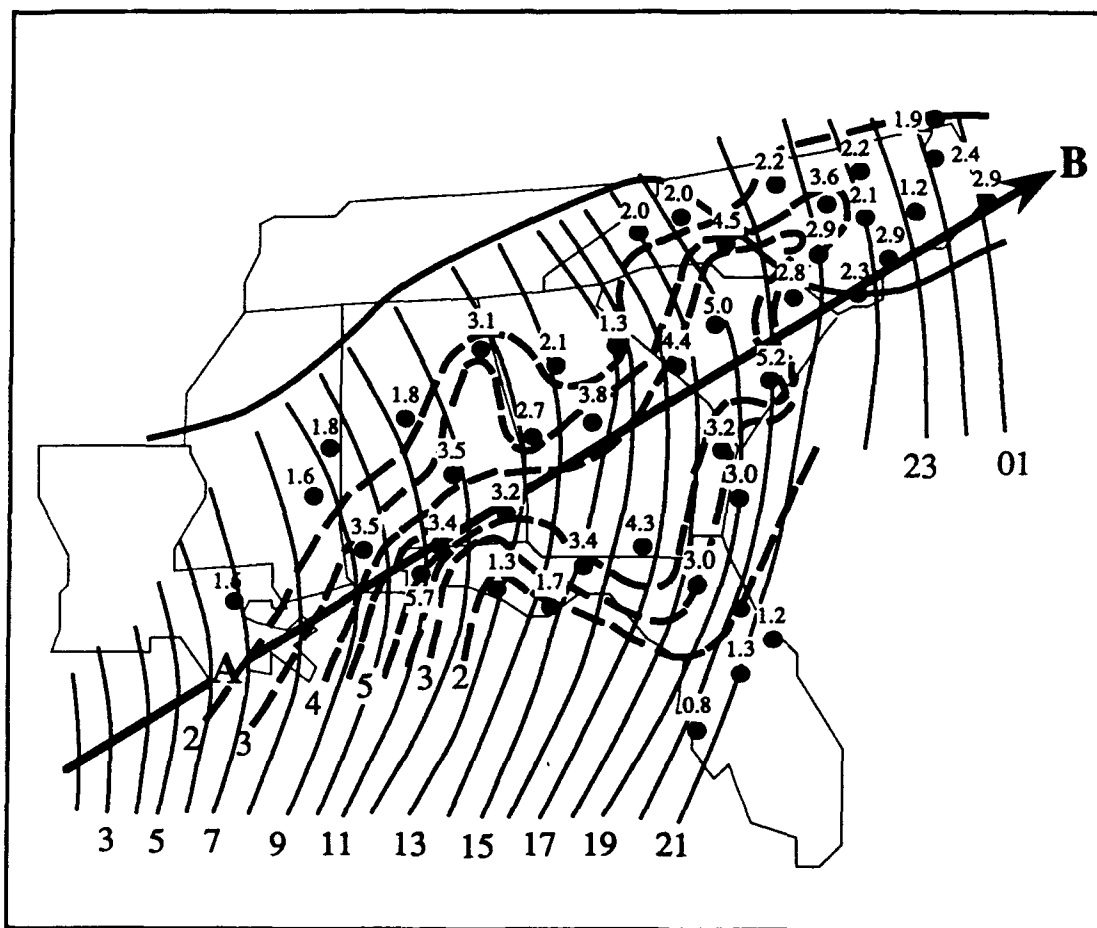


Figure 2.4 Wave propagation. Thin solid lines are isochrones of pressure trough (time in UTC shown at bottom). Individual reporting stations located at the dots show the reported pressure perturbation with wave passage. These values (mb) are isoplethted by the dashed lines. The locus of maximum perturbations is shown by the arrow. The heavy solid line is the local position of frontal boundaries with respect to the isochrone times.

minutes near point A increasing to about 2 hours at point B. The wave speed and half-periods indicate wavelength ranges of about 72 km near the Gulf coast to 346 km along the Carolina coast. Additionally, the timing of the trough passage and pressure perturbation magnitude at Augusta (AGS), GA match those at PAM II station 4 which is located just to the northwest. Thus, analysis over the GALE area based on the two data sets (GALE PAM II versus NWS hourlies) give consistent results.

To the west of point A in fig. 2.4, surface pressure perturbations that would have indicated wave passage were not found. Thus, the backtrack leads into the northwest Gulf of Mexico. At this point, information gleaned from the conceptual model presented in Chapter 1 (fig. 1.2) was used. That model, and a recent study of another gravity wave (Bosart and Seimon, 1988) showed an abrupt end in precipitation ahead of the trough line. Therefore, one would expect a definite signature of the wave in the precipitation field.

Figures 2.5 a-e show this signal in the radar precipitation throughout the wave's lifetime. The wave trough position at the time of each radar chart is shown and is based on fig. 2.4; a preceding squall line is also depicted.

Referring to fig. 2.4, it can be seen that the wave moves through the Slidell, LA. (SIL) area after 0700 UTC on the 6th. Figure 2.6a is the digitized radar for this site at 0727 UTC. Note the well-delineated western edge of the precipitation corresponding with the gravity wave's trough of lowest pressure.

Figure 2.6b is the SIL radar summary three hours earlier. The gravity wave (as shown by the sharp western edge of convection) is about 303 km distant to the west-southwest (240 degrees). If indeed the wave is moving along this line as shown in fig. 2.4, the movement over the next three hours (to wave passage at SIL) corresponds to a speed of 28 ms^{-1} , closely matching earlier results.

The radar composite at 0135 UTC (Fig. 2.7) has superimposed a backtrack timeline from Slidell assuming a 28 ms^{-1} speed. The satellite imagery during this time period reveals the initiation of strong convection by the cold front at a time and place (fig. 2.8) consistent with the time the gravity wave would be in this vicinity.

A more detailed investigation of the wave track in relation to the atmospheric structure will be presented in the next chapter. A related question raised by figure 2.4; namely that of the northern boundary of the wave, will also be discussed in the following chapter.

Based on the evidence thus far presented, it appears that the wave was generated in the vicinity of the northwestern Gulf of Mexico at about 0200 UTC on February 6.

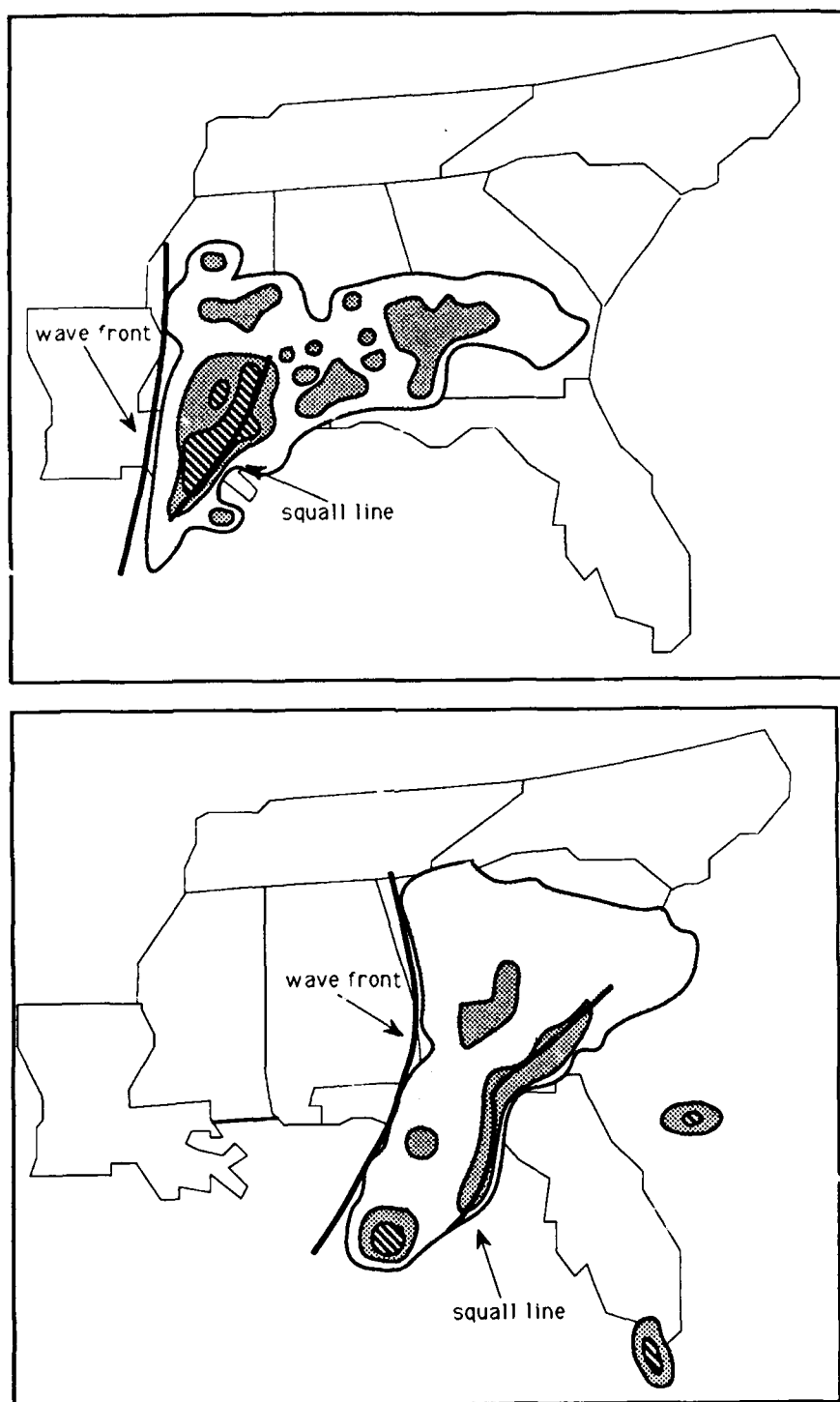


Figure 2.5 (a) Radar summary 0935 UTC 6 February 1986. (b) 1335 UTC 6 February.

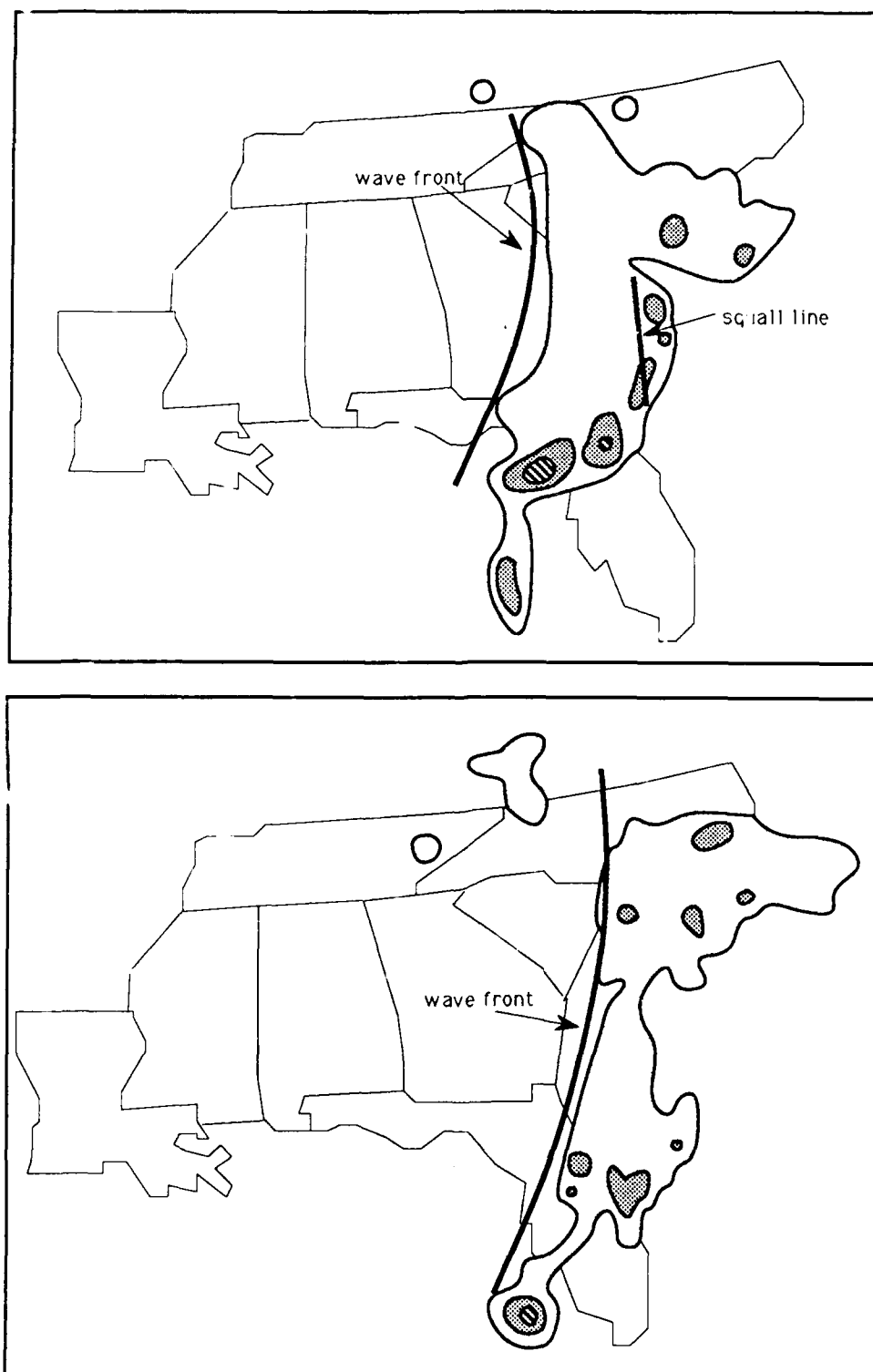


Figure 2.5 (c) Radar summary 1735 UTC 6 February 1986. (d) 2135 UTC 6 February.

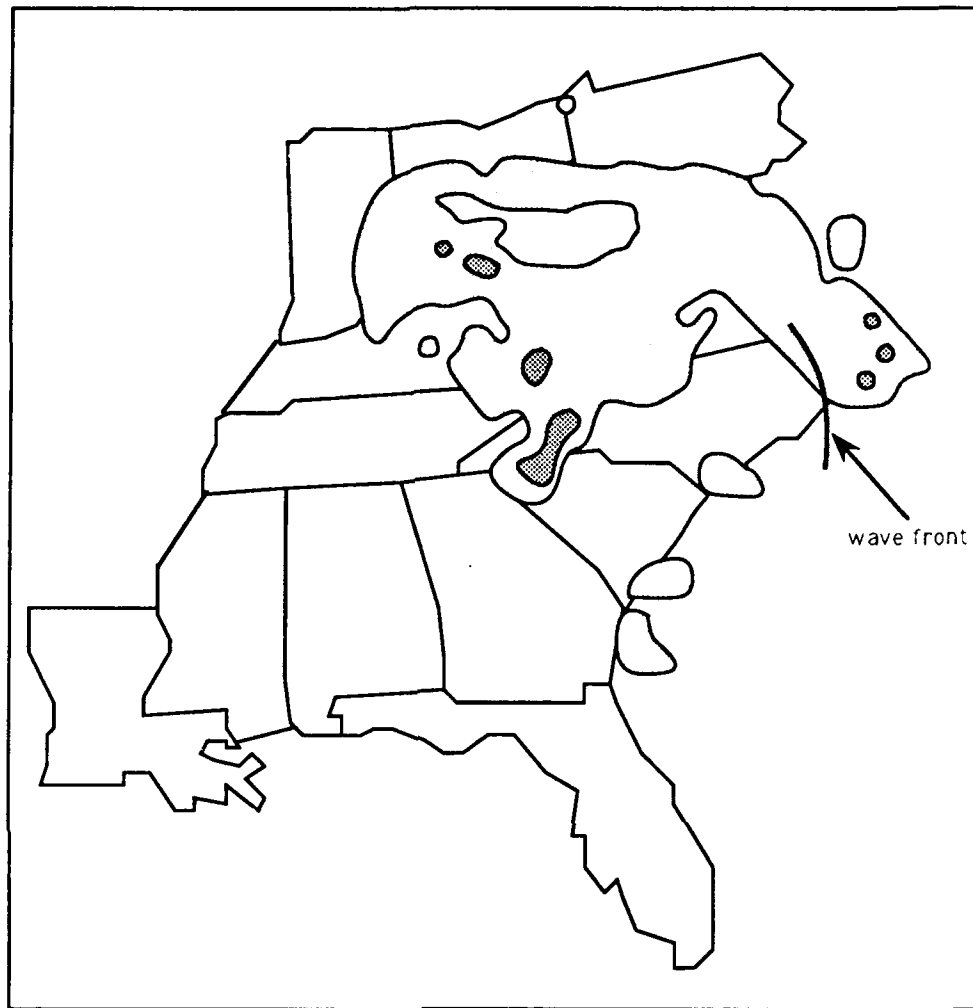


Figure 2.5 (e) Radar summary 0135 UTC 7 February 1986.

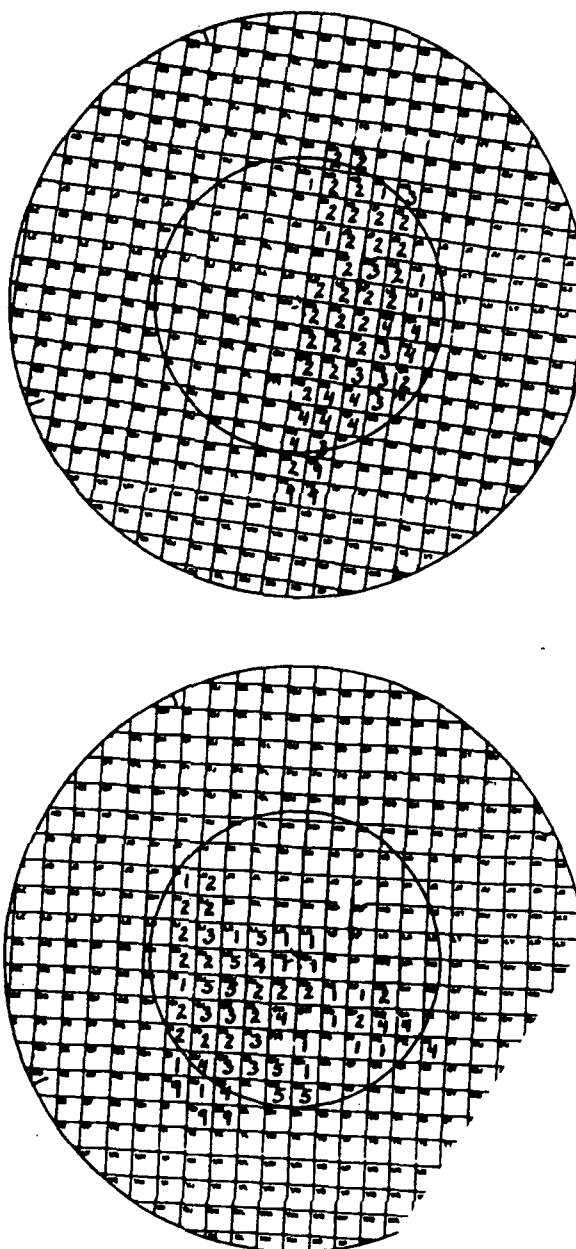


Figure 2.6 (a) Digitized radar summary from Slidell, LA 0727 UTC 6 February 1986. Numbers 1-9 indicate precipitation intensity levels, with 9 being "unknown". (b) Same as (a) except 0425 UTC 6 February.

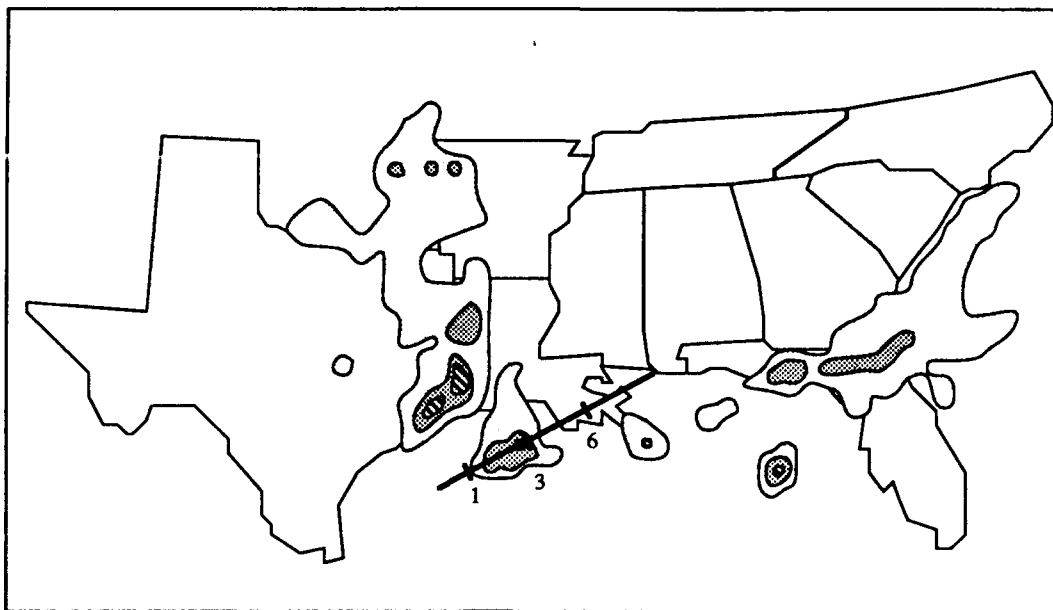


Figure 2.7 Radar summary 0135 UTC 6 February 1986. Backtrack timeline from Slidell, LA is shown.

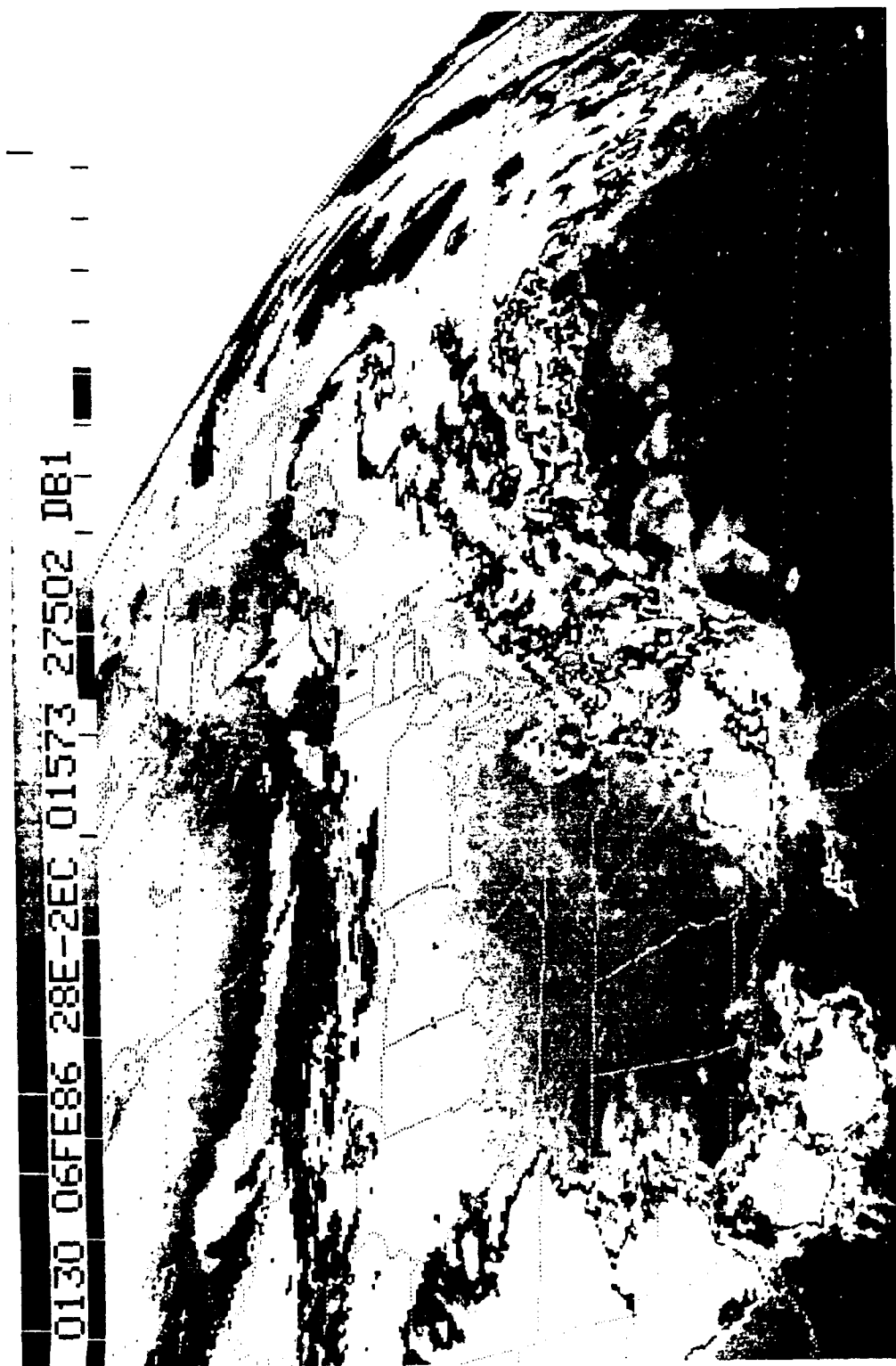


Figure 2.8 Geostationary Operational Environmental Satellite (GOES) infrared imagery at 0130 UTC 6 February 1986.

3. Wave Longevity

3.1 Atmospheric Ducting.

Gravity waves should propagate freely in the vertical. As mentioned earlier, this would lead to the wave losing energy so quickly as to be unrecognizable even one wavelength downstream. Since the wave under study was so long-lived, it must have been continually regenerated or else ducted. Raymond (1975) describes how a wave-CISK mechanism can form a significant source of energy for gravity waves. The generated waves organize convection which then produce more waves and so on. The other alternative, ducting, is explored here since locations north of the Gulf coast states did not experience thunderstorm activity.

A comprehensive theory on ducting has been developed by Lindzen and Tung (1976). The authors found that waves can exist (be ducted) for long periods of time and over great horizontal distances if a stable lower troposphere is capped by a layer above which effectively reflects the vertical propagation. In this situation there is only a small loss of wave energy, and continual forcing is not required.

For a layer of air to act as a duct, Lindzen and Tung showed that the layer must be statically stable. That is, the Brunt-Vaisala frequency squared, N^2 , must be positive;

$$N^2 = \frac{g}{\theta} \frac{\partial \theta}{\partial z}$$

Here, g is acceleration of gravity, θ is potential temperature, and z is the vertical coordinate. Additionally, the layer must be thick enough to contain one-quarter of the vertical wavelength and not contain a wind speed equal to the phase speed of the wave. If the latter were to occur a "critical level" would be situated in the duct and the wave would be completely absorbed (Booker and Bretherton, 1967). Note that the phase speed (C_d) in the duct is defined as $C_d = C - U_0$, where U_0 is the mean flow in the duct in the direction of wave propagation and C is the wave's observed phase speed.

Requirements for the upper and/or lower reflective layer are as follows:

i) The Richardson number must be < 0.25 either because the layer is sufficiently mixed so that the Brunt-Vaisala frequency is approximately zero or the layer is nearly saturated and conditionally unstable. The Richardson number is defined as:

$$R_i = \frac{g}{\theta} \frac{\partial \theta / \partial z}{\left(\partial u / \partial z \right)^2}$$

Here, $\partial u / \partial z$ is the vertical shear of the mean horizontal flow.

ii) The mean flow within the reflective region must equal C_d or come very close to it.

3.2 Vertical Atmospheric Structure.

In order to determine whether these requirements were met in the case under study, appropriate quantities were calculated at six locations along the wave path. Figure 3.1a shows the profiles of Richardson number (R_i) and Brunt-Vaisala frequency (N^2) for the Boothville, LA radiosonde taken at 0000 UTC 6 February. Calculations are based on the 10mb interpolated GALE sounding data. Some smoothing of the data was necessary. A low pass filter was used to eliminate wavelengths less than twice the original data spacing as is described in Shapiro (1975). If A_i represents a value at a central point in space, the smoothed grid value is obtained by

$$B_i = 0.25 A_{i+1} + 0.5 A_i + 0.25 A_{i-1}.$$

The wind shear calculations were obtained from the component of the wind in the direction of wave propagation (i.e., 240 degrees). The statically stable layer at Boothville extends from the surface to about 2,600 meters (740 mb). Note the layer near 700 mb where the air is weakly stratified. The Richardson number is < 0.25 and N is quite small.

The phase speed in the duct can be computed using the equation derived in Lindzen and Tung (1976). Noting that the ground itself serves as the lower reflecting surface where $C_d = C$, the equation becomes:

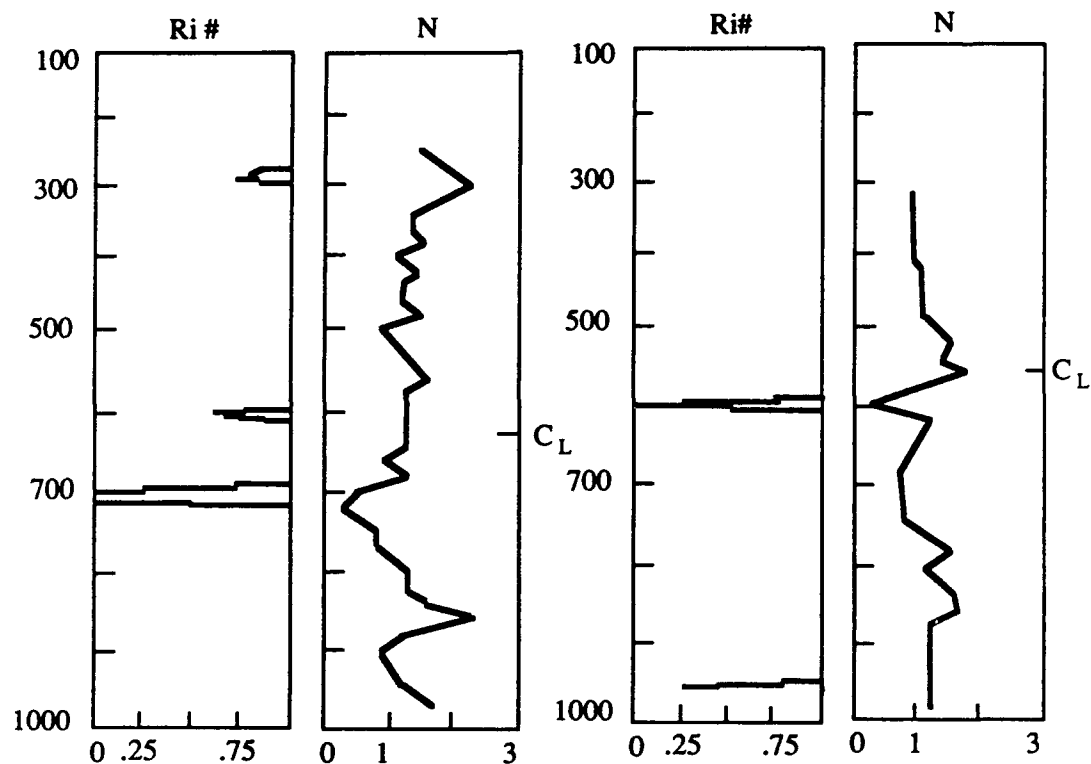


Figure 3.1 (a) Richardson number (Ri) and Brunt-Vaisala frequency (N) vertical profiles for Boothville, LA 0000 UTC 6 February 1986. (b) Same as (a) except for Apalachicola, FL 1200 UTC 6 February.

$$C_{d,n} \sim NH / \pi (1/2 + n).$$

Here N is the Brunt-Vaisala frequency, H the depth of the stable layer and n the vertical mode number. We will use $n=0$ (the longest vertical wavelength) since this is the wave that should be least affected by dissipative processes (e.g. friction) and hence dominate. Therefore,

$$C_d \sim 2NH / \pi.$$

For the Boothville sounding a mean value of $N=1.24 \times 10^{-2}$ was calculated within the duct that is 2,600 meters thick. This yields a phase speed of about 20.9 ms^{-1} . Note that the critical level is at 610mb. This is about 1 km higher than the level of minimum R_i . Given reasonable leeway due to measurement and calculation errors, the profile suggests the presence of a duct.

Next, consider the sounding from Apalachicola FL, (AQQ), at 1200 UTC 6 February (figure 3.1b). In this case the duct is 4,180 m thick ($N^2 > 0$ from surface to 610mb) with a mean N of 1.06×10^{-2} . At this site $C_d = 28.2 \text{ ms}^{-1}$. In this case, the critical level is located at 570 mb, very close to the weakly stratified layer as shown by the N profile.

Thus, it appears that a good duct is present along the Gulf coast in the area where the wave was initiated. Note that the wave was first seen strongly in the surface pressure data at Mobile, AL, which is right in this area. Also, the good agreement of the above calculations of C_d (especially for BVE) to that of the wave speed computed in Chapter 2 using the surface isochrones should be noted.

Figure 3.2 shows similar structure for four other stations along the wave path: Centerville, AL; Waycross, GA; Asheville, NC; and Beaufort, NC. In all cases, a well-defined duct is evident. It is therefore claimed that this structure is the reason that the wave propagated over such a great horizontal distance.

There are exceptions to this uniformity, however. At Athens, GA (Fig. 3.3) the duct does not extend down to the surface. Instead, the stable layer is bounded between 920 and 660 mb. At this location the ground is not within the duct, so that the phase speed C is given by $C_d + U_0 = C$. C_d at this station is 21.5 ms^{-1} and U_0 is determined to be 9.6 ms^{-1} . This produces a phase speed of 31.1 ms^{-1} . Referring back to figure 2.4, one can see in the isochrone spacing an apparent acceleration of the wave front in the

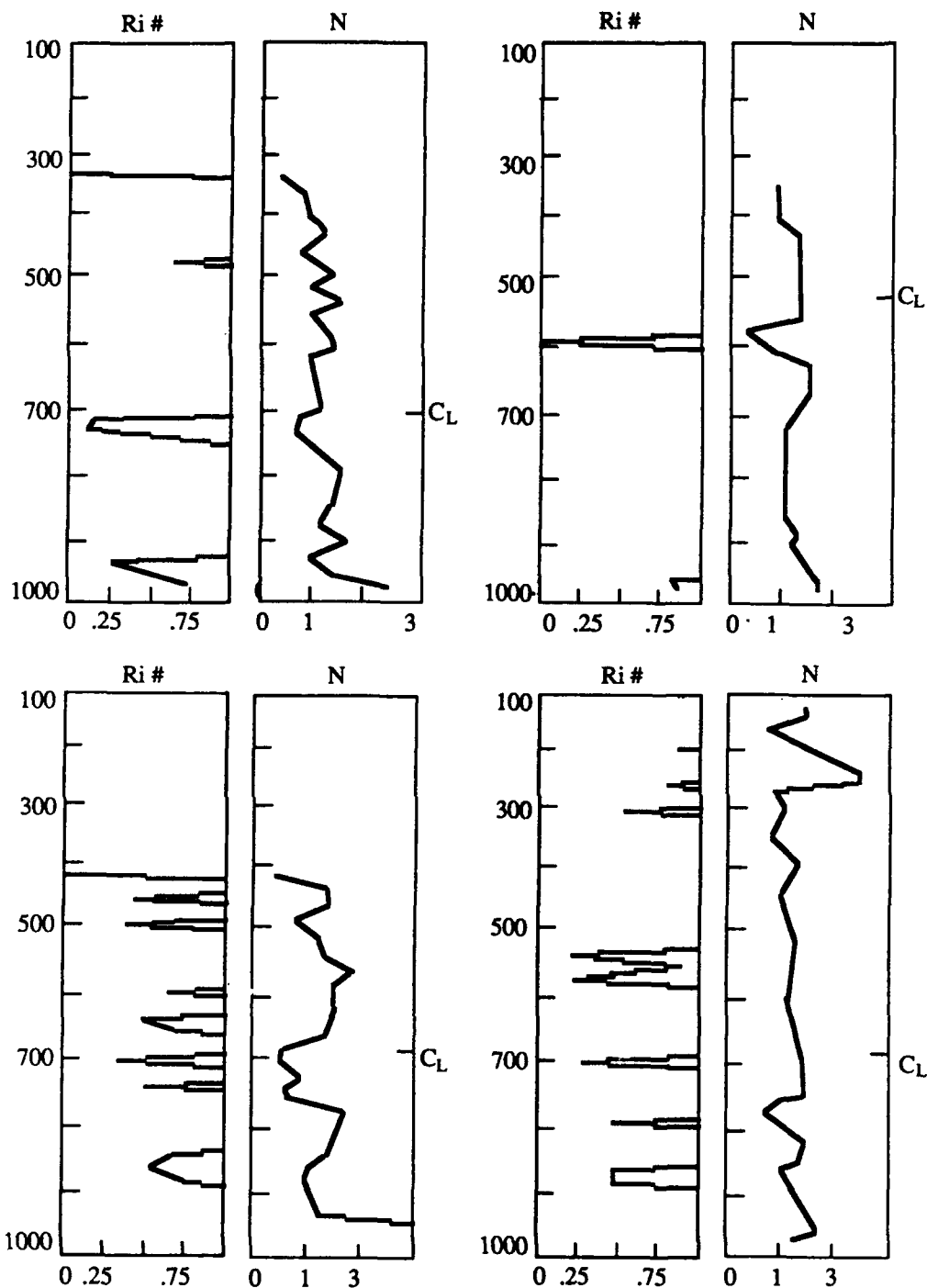


Figure 3.2 Same as figure 3.1 except for (a) Centerville, AL (b) Waycross, GA 1200 UTC 6 February 1986. (c) Asheville, NC 1800 UTC and (d) Beaufort, NC 2100 UTC 6 February.

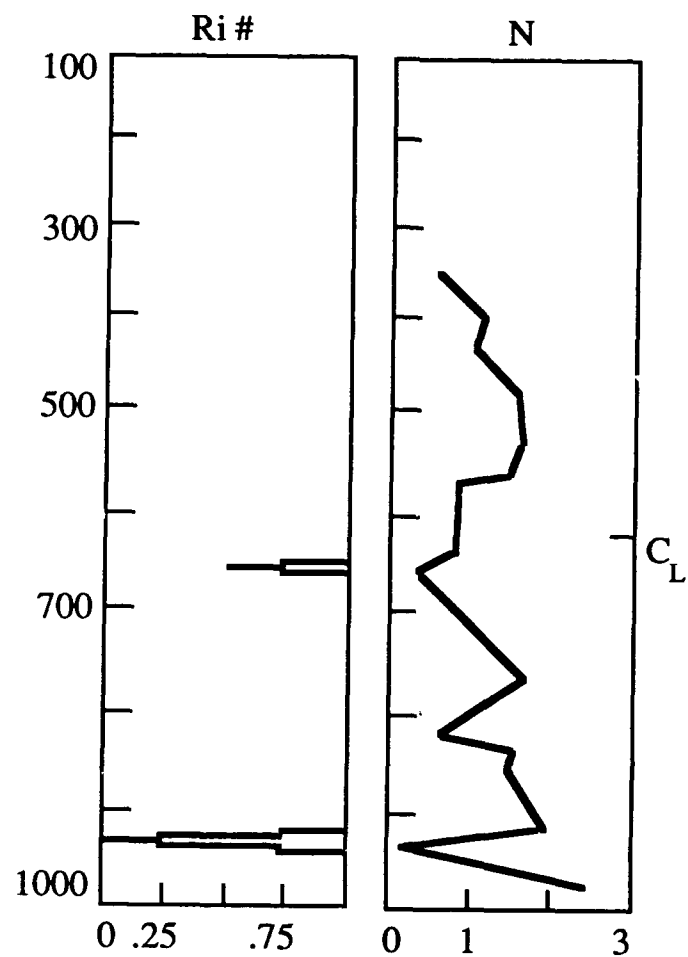


Figure 3.3 Same as figure 3.1 except for Athens, GA 1200 UTC 6 February 1986.

Athens area. Another interesting point in this sounding is the rather high critical level (480 mb), indicating energy leakage. This may account for the small pressure perturbation of 1.3 mb observed at that location.

Another question related to atmospheric structure involves the rather abrupt northern bound of the wave (fig .2.4). The reason for this must be related to the duct , that is, for some reason either the stable layer and/ or the weakly stratified capping layer is absent. Examination of the synoptic charts of 6 February leads to the hypothesis that the frontal structure was somehow involved - if only because of their coincidence with the wave boundary. Figure 2.4 shows the frontal positions in relation to the gravity wave's pressure trough.

It is appropriate to show the progress of the surface front. Figure 3.4 shows the quasi-stationary front over the PAM II network slipping southward with time as a back-door cold front (Carr, 1951) near the end of the wave episode (0000 UTC 7 February).

In the warm sector, all of the barograph traces available show a clear half-period (see for example Columbia, SC, figure 3.3) of 20-40 minutes. In contrast, the barograph traces of stations experiencing wave passage in the cold air north of the back-door cold front show much longer half-periods. At Elizabeth City, NC (ECG), for example (fig.3.5) the half-period is about two hours.

The frontal zone has clearly disrupted the ducting structure; the longer half-periods are indicative of wave dissipation. Further evidence of this point is provided in figure 3.6. This sounding is from Petersburg, VA and shows the loss of the duct's capping layer in the cold air thus allowing energy leakage and dispersion.

It should be noted that the northern edge of the gravity wave first encountered the front in North Carolina between 1900 and 2000 UTC. Therefore, most of the PAM II stations were in the cold air at the time of wave passage. This is consistent with DeMaria et al's (1989) finding of a 1 to 2 hour half-period in this region.

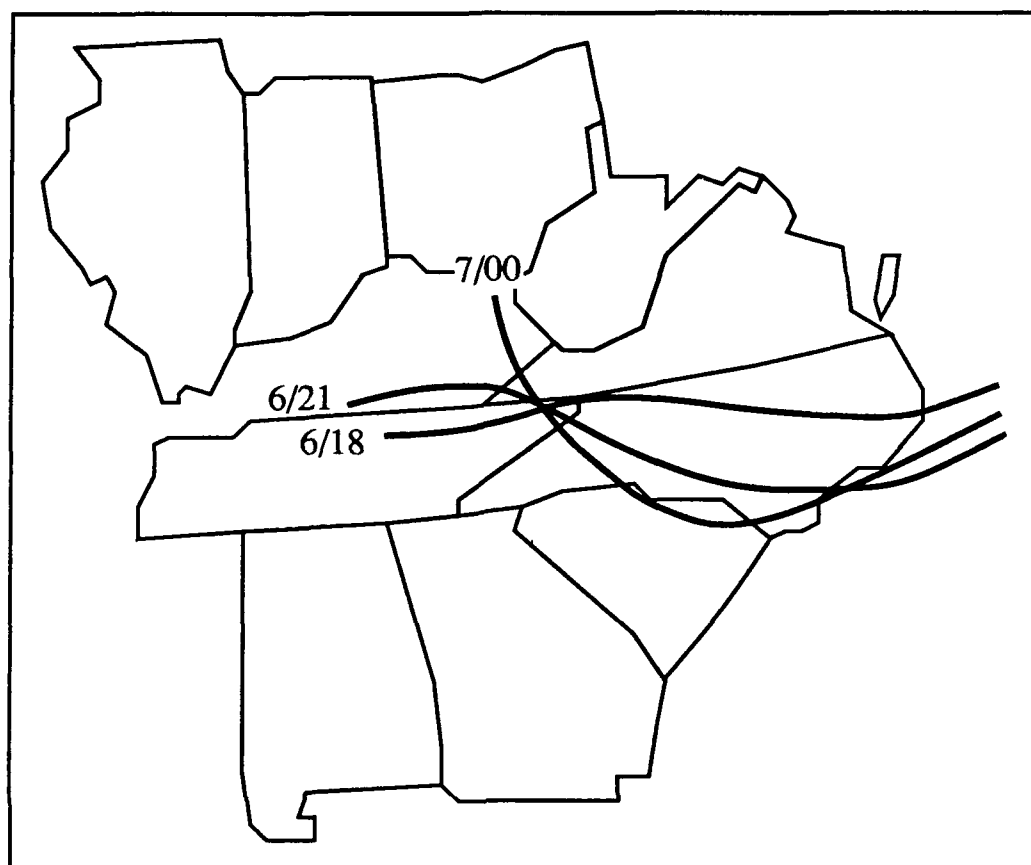


Figure 3.4 Position of "back-door" cold front at 3-hour intervals from 1800 UTC 6 February 1986 until 0000 UTC 7 February 1986.

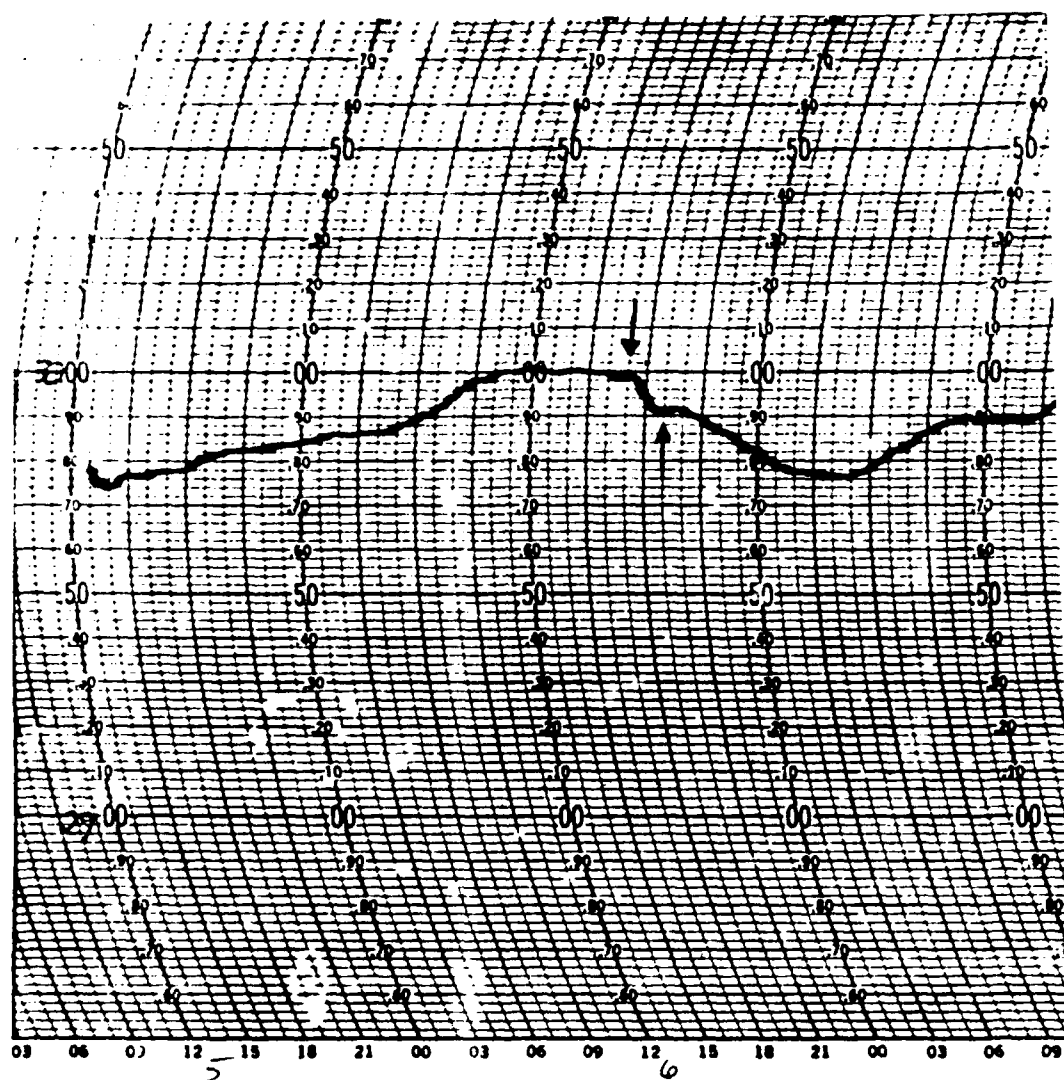


Figure 3.5 Barogram from Elizabeth City, NC. Time scale of trace is from 5 February 1300 LST until 7 February 1530 LST. Note gravity wave signature on 6 February from 1700-1900 LST.

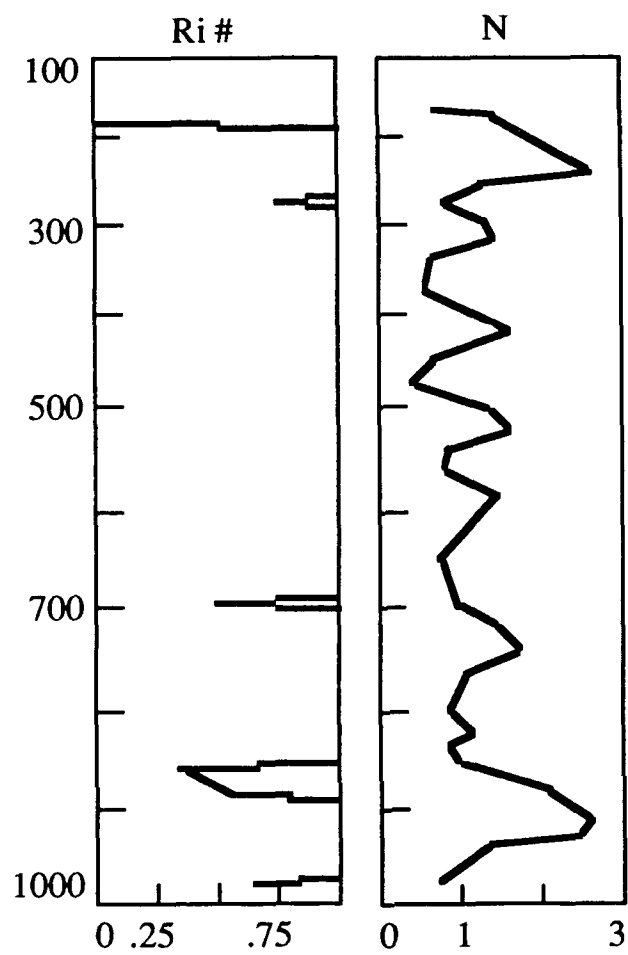


Figure 3.6 Same as figure 3.1 except for Petersburg, VA α

4. Wave Initiation

Gossard and Hooke (1975) list five source mechanisms for mesoscale gravity waves. They are: orographic forcing; shear instability; geostrophic adjustment processes; density impulses (accelerating fronts); and convection. Each of these possible initiators will be briefly reviewed and then examined, using the synoptic setting as a guide, in order to isolate the most likely trigger for the gravity wave of 6 February 1986.

4.1 Orographic Forcing.

As the name implies, this type of gravity wave initiation requires a mountain range - which is obviously not present over the Gulf coast states. Air parcels forced over the mountain in a statically stable atmosphere will be displaced from their steady state positions and undergo buoyancy oscillations. The structure of the atmosphere determines the resultant wave mode, while the exact shape of the terrain dictates the strength applied to each wavelength.

Although the Sierra Madre mountains of northern Mexico can be found to the west of the wave source region, a gravity wave so produced would have been seen in the surface pressure field over western Louisiana and perhaps southeastern Texas. It was not. Additionally, a ducting structure like that discussed in Chapter 3, did not exist over this region.

4.2 Shear Instability

Gravity waves can be generated if air parcels, displaced from their equilibrium position, gain kinetic energy from the background flow (Hooke, 1984). This situation can be quantified by the Richardson number (R_i), which was described in Chapter 3. This parameter represents the ratio of the energy extraction from the buoyancy force to the energy gained by the mean shear.

It has been postulated that the majority of gravity wave events during the winter months (when convection is at a minimum) is caused by this phenomenon (Gedzelman, 1983). Of particular significance in the current study, however, are Gedzelman's findings that even though shear generated waves are apparently non-dispersive, they do not travel far from their source region and have very small amplitudes (fig. 4.1). Based on this work, it is unlikely that the 6 February 1986 wave was generated by shear instability.

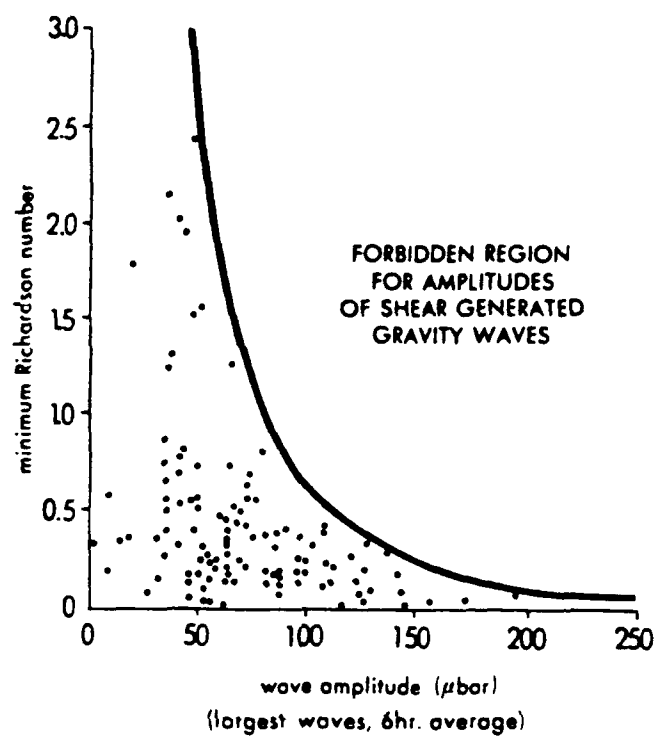


Figure 4.1 Wave amplitudes as a function of minimum Richardson number. The envelope indicates that large-amplitude waves are not excited by shear instability. (After Gedzelman and Rilling, 1978).

Another interesting connection between shear instability generated waves and their environment are the correlations between amplitude, maximum wind speed aloft and static stability. Gedzelman found a correlation coefficient of 0.914 between wave amplitude and the product of maximum wind speed aloft and static stability (as expressed in terms of the potential temperature difference) between 700 mb and the surface.

For the present case, a similar statistical investigation was undertaken. Thirteen radiosonde stations were available along the wave path which also had surface pressure perturbation (amplitude) data. All soundings were chosen such that they were the closest in time to just prior to wave passage. The correlation between pressure amplitude and the product of maximum wind and static stability was found to be $-.05$. Thus, less than 1% ($.05$ squared = $.0025$) of the variation in pressure perturbations is explained by the product of maximum wind and stability.

These results indicate no relationship between shear and wave amplitude. Based on the above discussion, it is the opinion of the author that shear instability could not be responsible for the 6 February 1986 gravity wave.

4.3 Geostrophic Adjustment

Recently, Uccellini and Koch (1986) summarized thirteen different case studies involving waves that possessed the following properties: periods > 1 hr., horizontal wavelengths > 50 km and surface pressure perturbations > 0.2 mb. They point out that although the authors of the individual studies cite differing initiating mechanisms, all of the cases appear to develop within a common synoptic setting. Furthermore, in all of these instances the wave duration was long (shortest was 9 hours; longest 33+ hrs.) and there is a significant impact on the sensible weather (wind, cloud, precipitation).

The synoptic situation described in chapter 2 compares favorably with the other cases just described. All of these situations have an upper-level trough-ridge pattern superposed on a surface low with fronts and warm sector in the same relative position as the present case. Uccellini and Koch argue that the most likely mechanism for gravity wave formation is the geostrophic adjustment associated with the upper-level jet streak.

Large scale, mid-latitude flow is nearly in hydrostatic and geostrophic balance. However, this balance of forces can be upset. For instance, an addition of momentum to a rotating fluid can cause a local geostrophic imbalance (Uccellini and Koch, 1986). The balance may also be disrupted by the flow itself through processes which disturb the thermal wind balance (Hoskins et al., 1978).

It must be noted, however, that the balance is continually re-established by ageostrophic circulations. Thus, the atmosphere is never very far from geostrophic and hydrostatic balance on the synoptic scale. This principle of quasi-geostrophic theory can be qualitatively shown in a number of ways. One particularly clear example is discussed by Bluestein (1986) in the vicinity of a straight line jet streak (figure 4.2). This figure illustrates the idea that as an air parcel decelerates in the exit region of a jet it loses kinetic energy and gains potential energy. The result is convergence to the right and divergence to the left of the jet axis. The vertical motions associated with this divergence field complete the ageostrophic circulations.

There are instances where the quasi-geostrophic circulations described may not be sufficient. In particular, Uccellini and Koch (1986) argue that geostrophic imbalance is quite pronounced when a jet streak (source of momentum) approaches an inflection point in the flow field. In this situation, numerical work (Kaplan and Paine, 1977) has shown that large increases in divergence occur in the right exit region of the jet. To re-establish the geostrophic balance, gravity waves may be shed by the jet (Van Tuyl and Young, 1982). When this occurs, numerical model results of Van Tuyl and Young show that the typical "four corner" vertical velocity pattern (figure 4.3a) is lost, and another pattern develops in the vertical velocity field, which is a reflection of the disturbed divergence field (figures 4.3b,c).

If the gravity wave were the result of geostrophic adjustment in this study, one would expect to see a disrupted exit region, perhaps resembling the latter two figures. The divergence field at jet stream level for the present case is shown in figure 4.4. This field was obtained from second-order centered differences applied to objectively analyzed wind components at grid points (see Appendix 1). The symmetrical position of the convergence-divergence pairs across the jet axis more closely resembles the pattern in figure 4.2a and the expected vertical velocity pattern in figure 4.3a than the patterns in figures 4.3b,c. The symmetry across the axis in figure 4.4 suggests that the flow is in geostrophic equilibrium and gravity waves should not be expected as a result of a geostrophic adjustment process.

4.4 Density Impulses (Accelerating Fronts).

An accelerating surface front can also upset atmospheric geostrophic and hydrostatic balance. A front can be defined as the boundary separating air masses of different densities (Byers, 1974). In the cold season especially, the leading edge of an

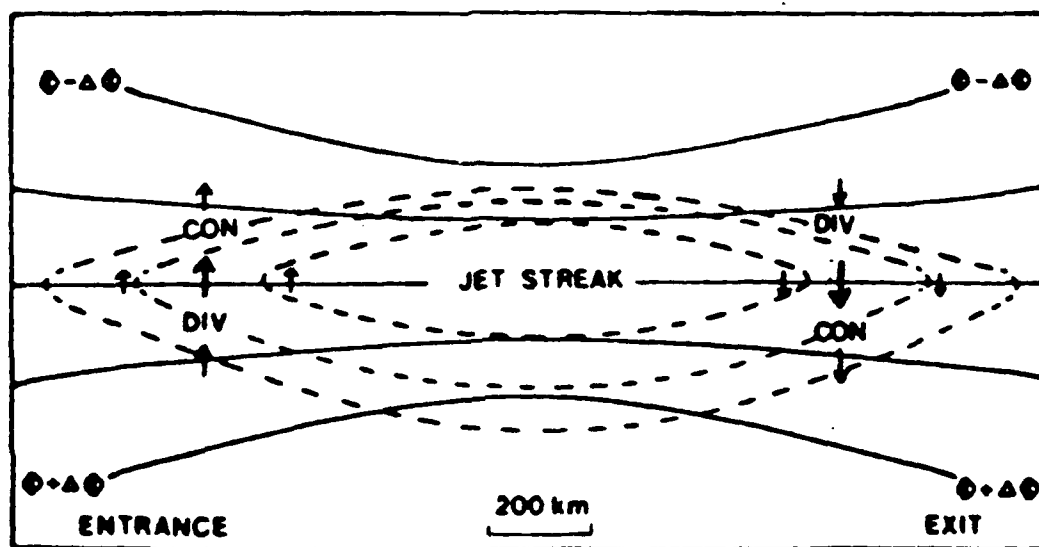


Figure 4.2 The ageostrophic motions (arrows) and associated convergence (CON) and divergence (DIVERGENCE) patterns in the vicinity of a jet streak. (From Bluestein, 1986).

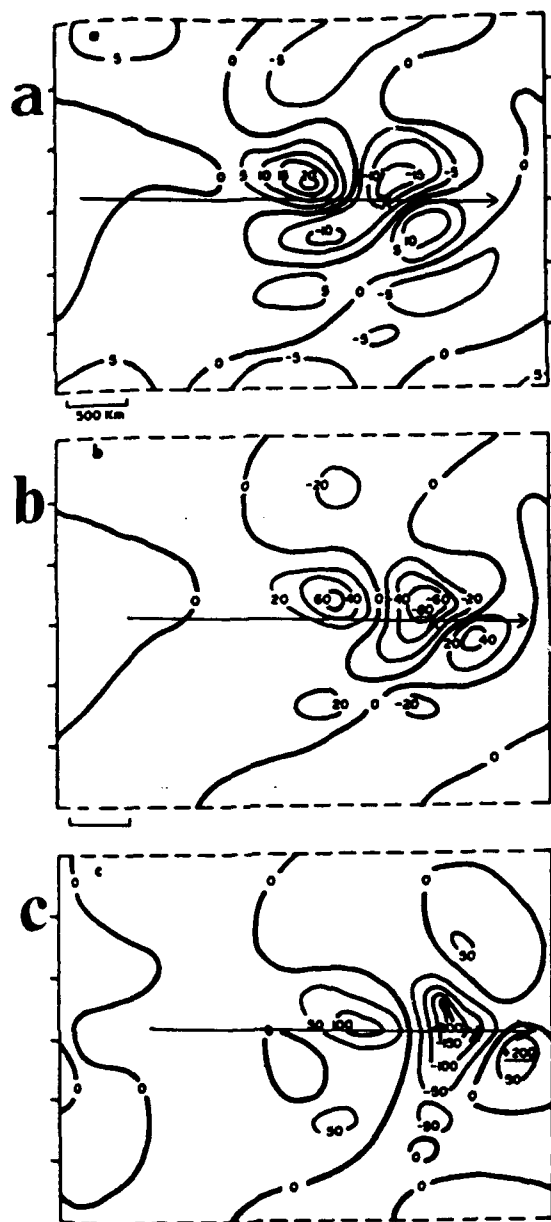


Figure 4.3 (a) 600 mb vertical velocity (10^{-5} S^{-1}) at 12 hours into three numerical models. Mean flow is left to right. Jet core location at 400 mb is marked with an X. (b) divergence field for experiment in (a). (c) Same as (b). (From Van Tuyl and Young, 1982).

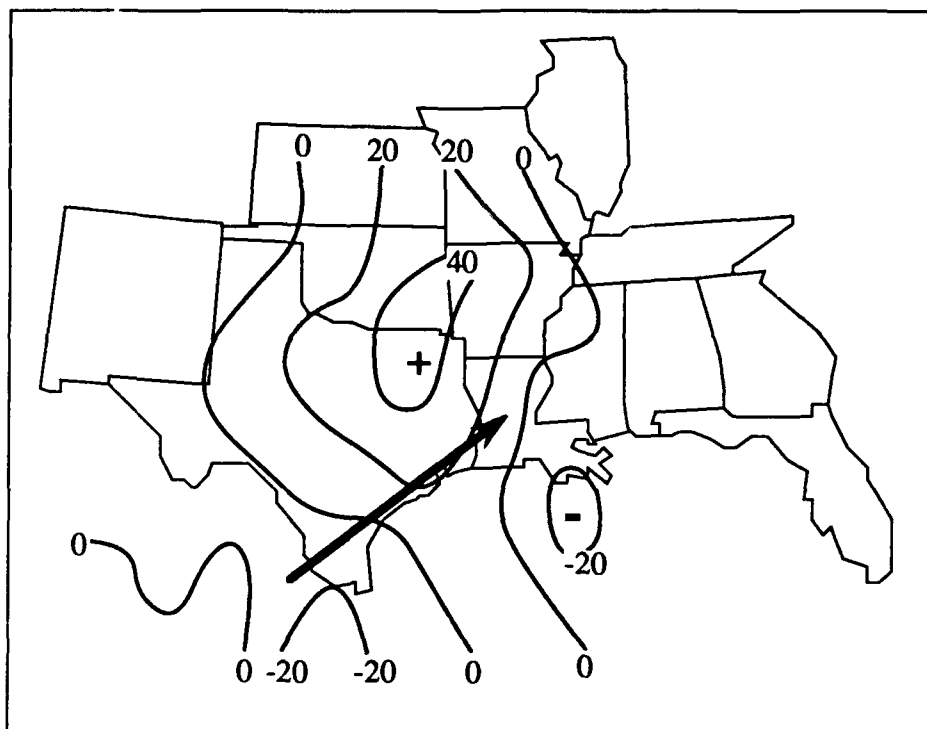


Figure 4.4 Horizontal divergence (10^{-6} S^{-1}) at 300 mb 0000 UTC 6 February 1986. Jet streak location indicated by the arrow.

accelerating polar air mass can vigorously displace the warm air ahead of it. This sudden forced ascent of the warm air sends out density impulses in a statically stable layer. If the warm air contains a marked inversion layer, a gravity wave of large amplitude will propagate from the source along the inversion.

Figure 4.5 shows the position of the cold front described in Chapter 2 every three hours between 5 February 1800 UTC and 6 February 0600 UTC. There is a lack of a vigorous cold outbreak with this front (fig. 2.1a) and thus a good physical "push" does not exist. Furthermore, since the frontal boundary (especially in the western Gulf of Mexico) is not accelerating, there is no reason to believe that this caused the gravity wave of interest here.

4.5 Convection

Thunderstorms are known to generate gravity waves at various levels in the atmosphere from the surface up into the ionosphere (Balachandran, 1980). The local energy source of these waves is far from clear, and numerous conceptual and mathematical models have been proposed (e.g., Smith and Lin, 1982). An illustration of one simple conceptual idea is given in fig. 4.6. Here, penetrative convection is shown. The thermal updraft associated with the thunderstorm cell acts as a point source for gravity waves when it encounters stable overlying air (Hooke, 1984). It follows that the stronger the impulsive force of the convection, the greater the amplitude of the secondary disturbance. Satellite imagery has provided spectacular photographs of this type of wave forcing. The reader is referred to Erickson and Whitney (1973) for examples. A related idea involves the release of latent heat during the convection. This wave-CISK (Conditional Instability of the Second Kind) idea is explained in Lindzen (1974) and Raymond (1975), and may play a role in this case by initially organizing the convection into a sharp band.

At 1730 UTC the northwestern Gulf of Mexico is quiet in regards to thunderstorm activity (Figure 4.7a). By 1930 GMT satellite imagery shows a shallow line of convection located over southeastern Texas and the northern Gulf of Mexico (fig. 4.8). There is also an area of cumulus with some vertical extent further to the southeast (26° N, 92° W). Figure 4.7b is the corresponding radar summary chart, which indicates a maximum top of 11,500 meters south-southeast of Galveston, Texas.

Over the next six hours the convection intensifies (Figs. 4.9 - 4.11) until the maximum tops have reached over 15,000 meters. At 0000 UTC 6 February the tropopause was reported at 9,500 meters at Jackson, MS; 9,250 meters at Lake Charles,

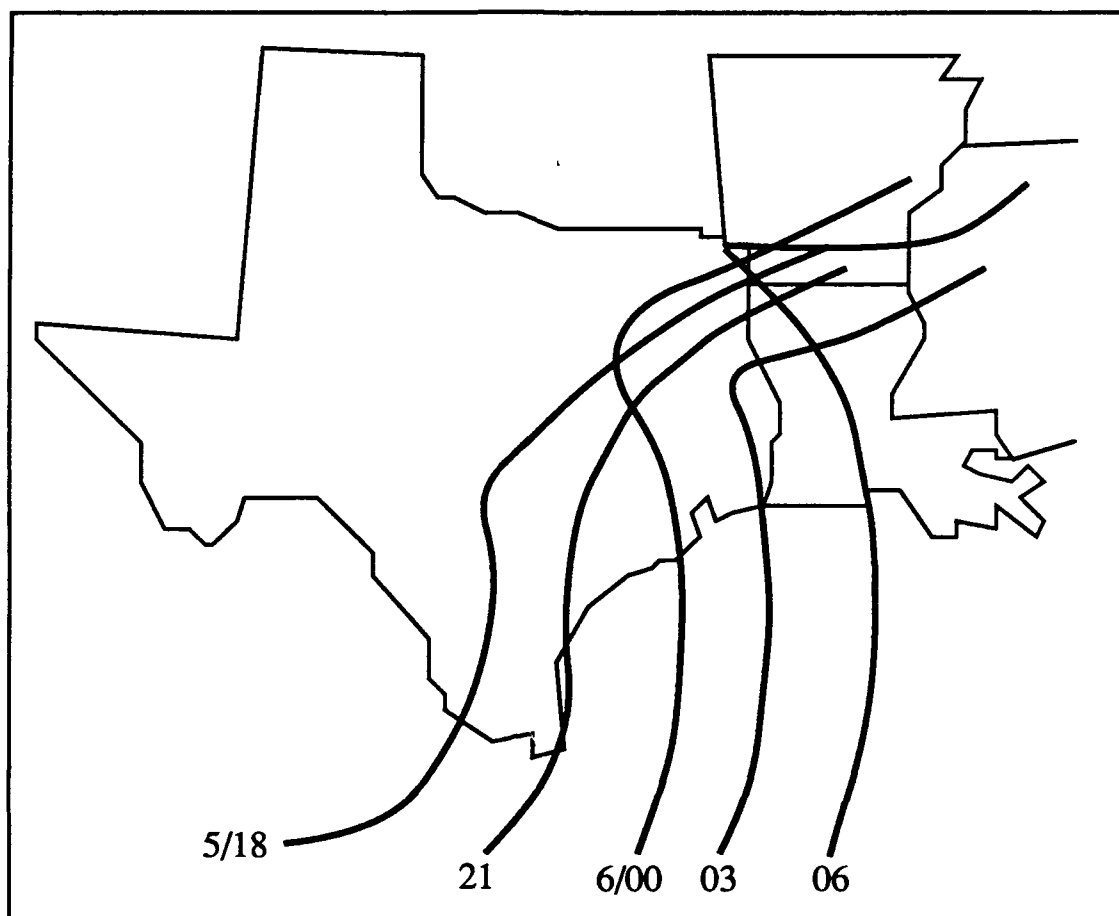


Figure 4.5 Position of frontal system at 3-hour intervals from 5 February 1800 UTC until 6 February 0600 UTC.

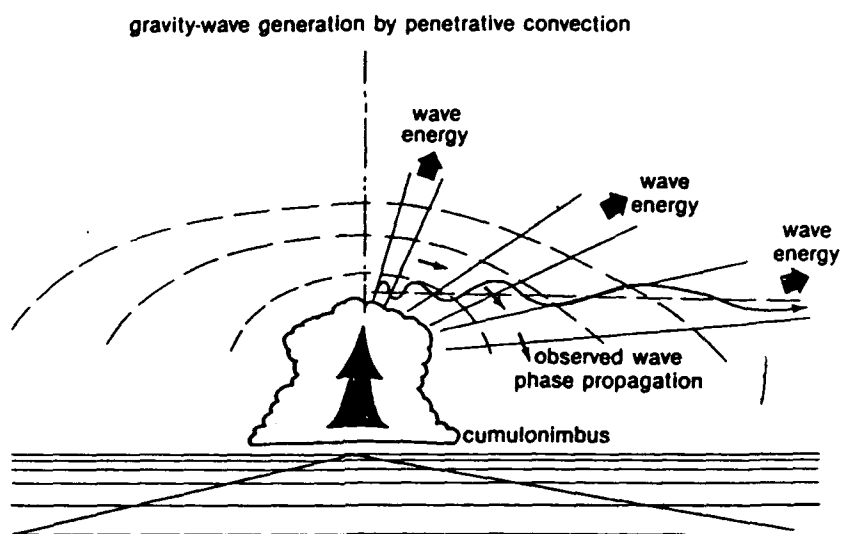


Figure 4.6 Gravity-wave generation by penetrative convection. (From Hooke, 1984).

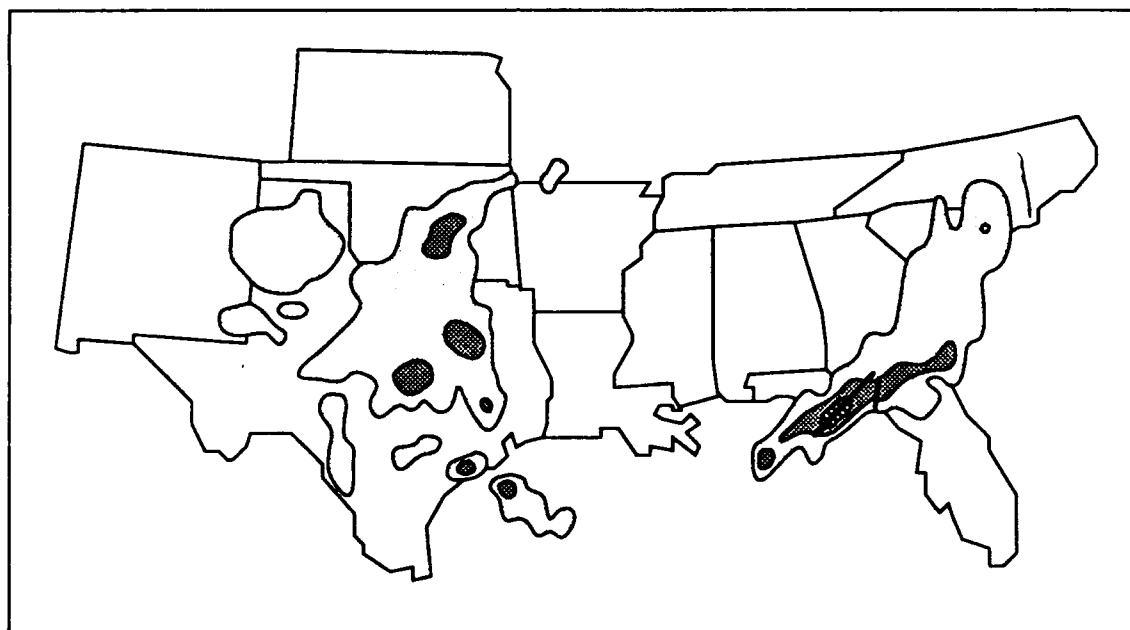
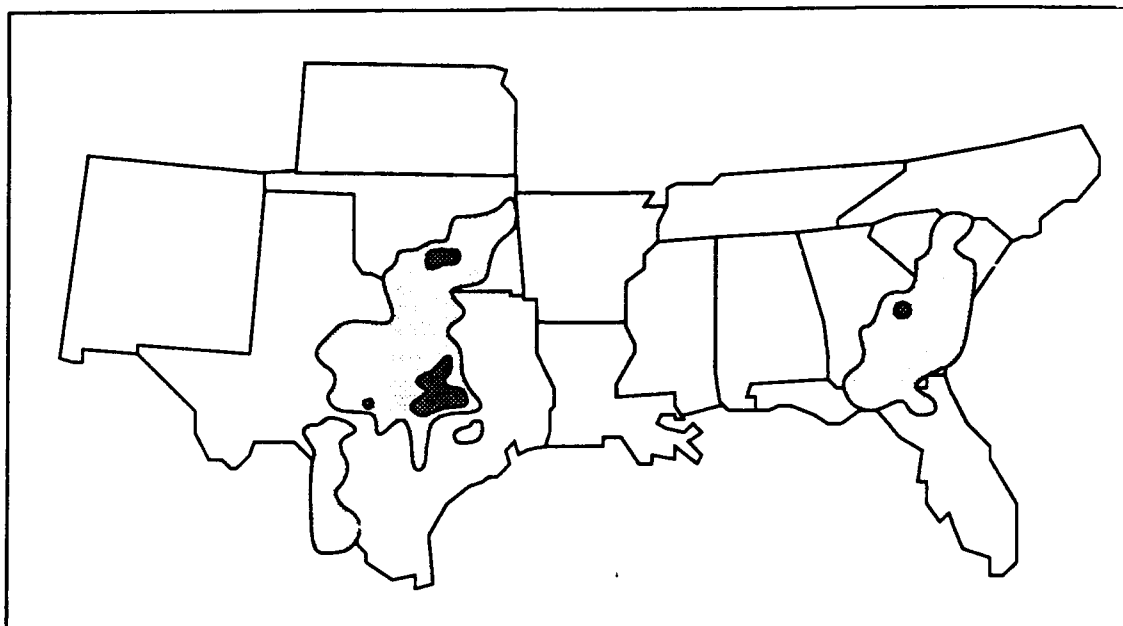


Figure 4.7 (a) Radar summary 1735 UTC 5 February 1986. (b) Same as in (a) except for 1935 UTC 5 February.

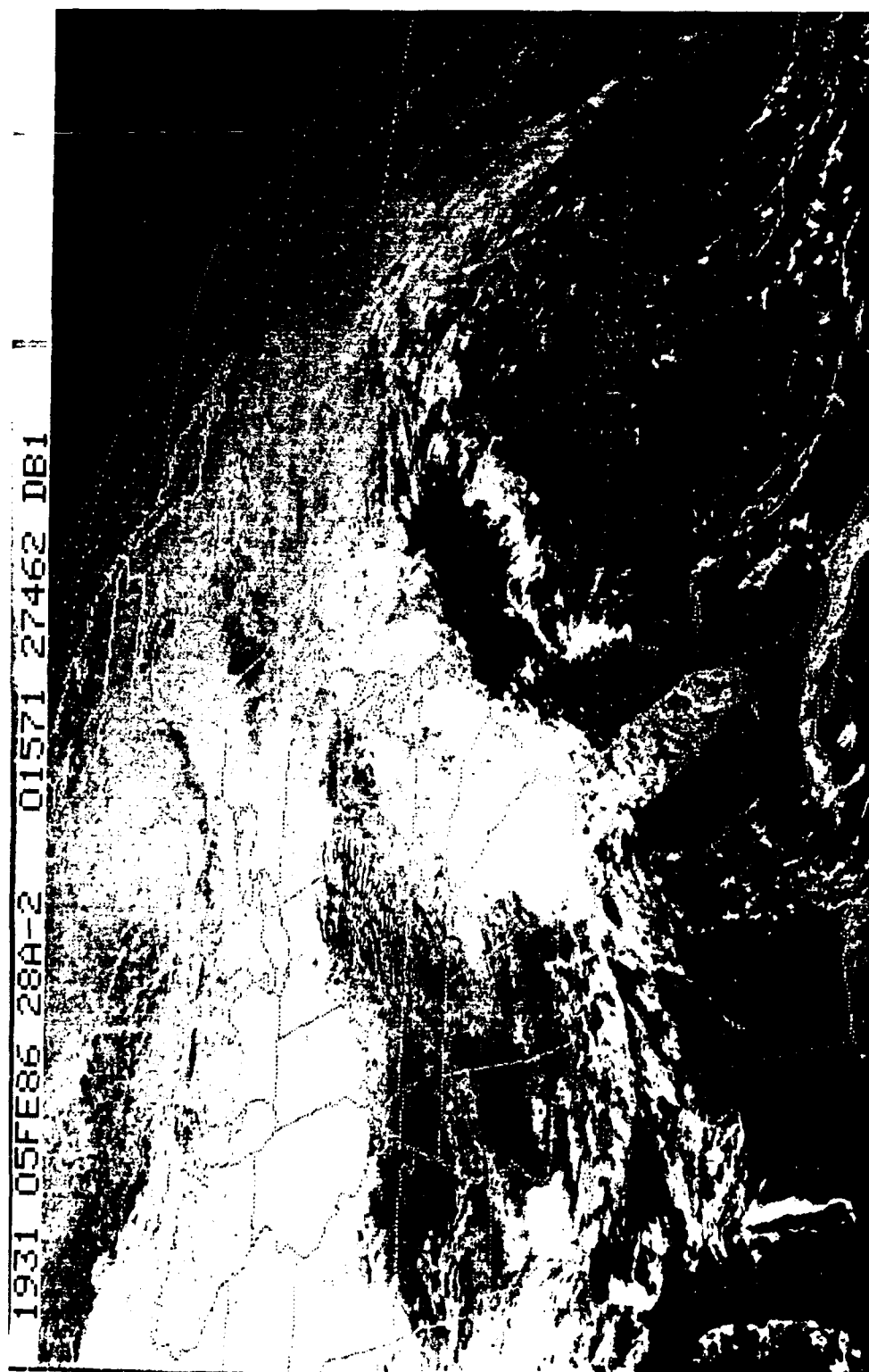


Figure 4.8 Same as Figure 2.8 except visible imagery at 1930 UTC 5 February 1986.

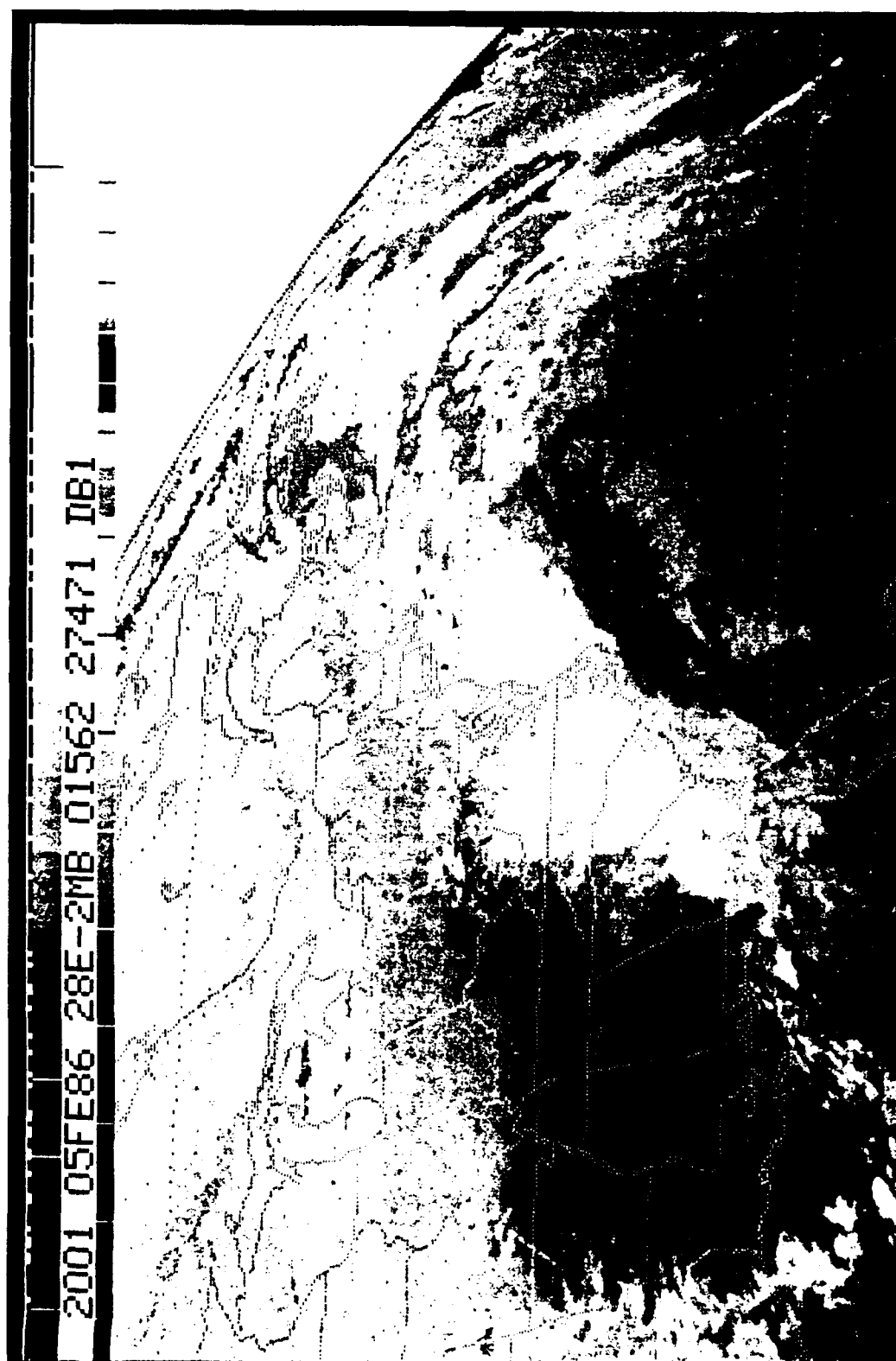


Figure 4.10 Same as Figure 2.8 except at 2200 UTC 5 February 1986.

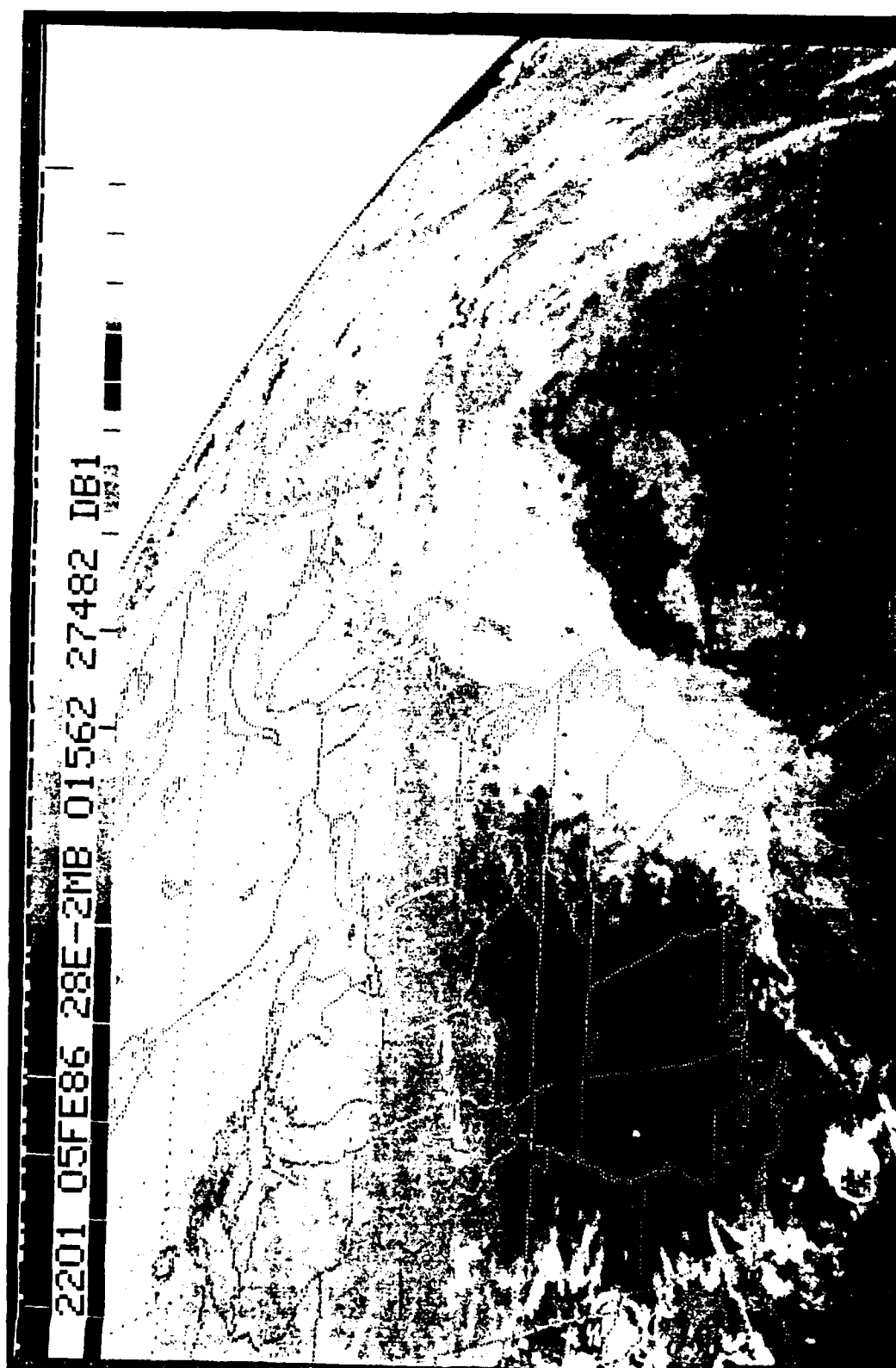


Figure 4.9 Same as Figure 2.8 except at 2000 UTC 5 February 1986.

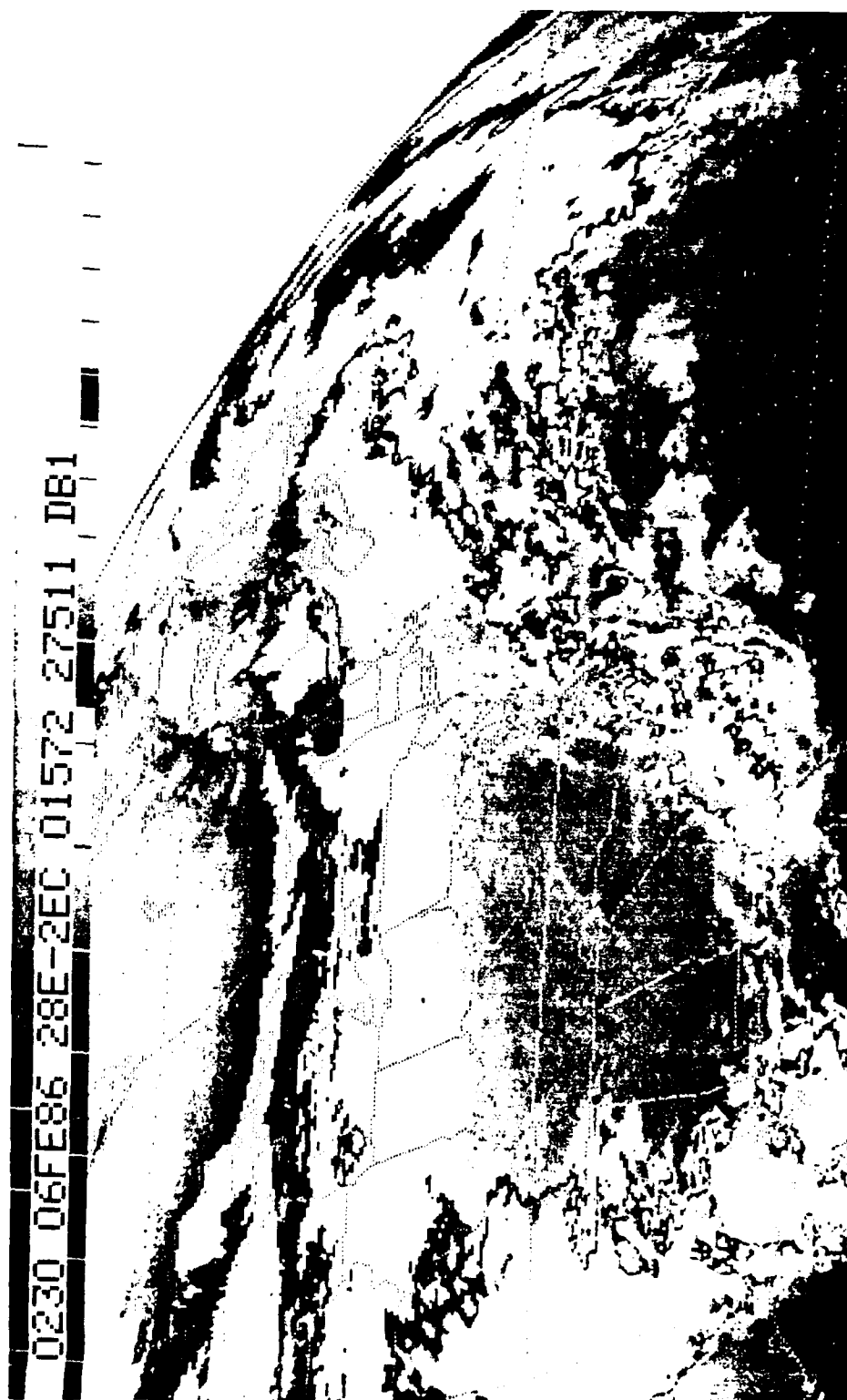


Figure 4.11 Same as Figure 2.8 except at 0230 UTC 6 February 1986.

LA and 8,500 meters at Boothville, LA. The thermodynamic diagram for Boothville (BVE) is shown in fig. 4.12. A strong inversion (approx. 900-800mb) caps a warm, moist lower troposphere. If the air in the surface layer beneath the inversion were to be lifted to the top of the inversion it would be free to rise all the way to the tropopause. Low level warm advection or solar heating (since it is 1800 LST) is unlikely to provide the required initial lift. The approaching cold front (described in Chapter 2) however; does provide a good source of mechanical lifting.

The intensification of the thunderstorm activity towards 0000 UTC 6 February coincides with positive vorticity advection aloft over the region (see fig. 2.1b). This serves to enhance the convection by providing added lift. Radar observations from Lake Charles, LA indicate the explosive nature of the storms - it takes only 25 minutes for a cell to reach the stratosphere!

This positive evidence, coupled with the unlikely importance of the other four gravity wave source mechanisms, has led the author to conclude that the dramatic onset of deep convection in the northwestern Gulf of Mexico to be the cause of the 6 February event.

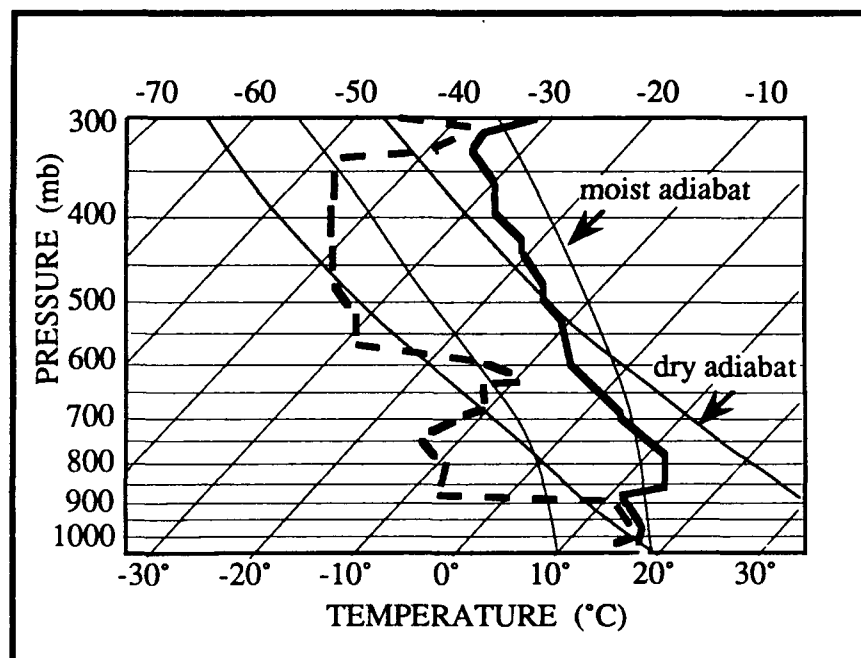


Figure 4.12 Skew-T Log-P diagram for Boothville, LA at 0000 UTC 6 February 1986. Temperature and dew point are indicated by the bold solid and dashed lines respectively.

5. Discussion and Conclusions

During the Genesis of Atlantic Lows Experiment (GALE), a three-day period from 4 to 6 February 1986 was analyzed by DeMaria et al. (1989) for the occurrence of gravity waves. Four cases were identified; the most well-defined of which moved through the PAM II network late in the day on the 6th. This was also the only case in which the precipitation field was clearly associated with the movement of the wave. Furthermore, the results showed that this wave was freely propagating with an unknown source outside and westward of the PAM II network.

Using surface pressure perturbations based on microbarographs and hourly surface data to identify the wave trough; the wave was traced backwards in time to the northwestern Gulf coast. This analysis revealed a solitary wave of depression (negative perturbations of 2-5 mb) with a mean propagation speed of 24 m/s, a half-wavelength of 36 - 170 km and half-period of 25min to 2 hours. These results matched the wave characteristics as computed by DeMaria et al. over the PAM II network - confirming that the wave indeed had a distant origin.

The source mechanism of the wave investigated formed within a synoptic setting similar to that of 13 other gravity wave case studies (Uccellini and Koch, 1986). A jet streak at 300 mb which had rotated around the base of a longwave trough was approaching the inflection point between the trough and the downstream ridge. At the surface, a low pressure system with its associated frontal structures began to deepen over the northwest Gulf of Mexico as the jet streak and its associated vorticity advection moved overhead. This scenario resulted in strong convection after 6 February 0000 UTC near the Louisiana and Alabama coast - where the gravity wave was first detected.

Five possible initiators of the wave were discussed: orographic forcing; shear instability; geostrophic adjustment; density impulses; and convection. The orographic gravity wave scenario is not likely here due to the lack of a ducting structure over southeastern Texas. Shear instability is judged unlikely as an energy source based on negative results of the statistical correlations between wind speed and static stability. Gravity waves ejected from a region undergoing geostrophic adjustment are also unlikely. The 300 mb jet streak, likely to be the cause of the adjustment process, is found to be in quasi-geostrophic balance. A density impulse associated with the surface cold front was also ruled out - the front did not have the required acceleration.

The most likely mechanism for creating the 6 February gravity wave was the deep, impulsive convection previously mentioned. The oscillatory time scale of this forcing was shown to have a half-period that matched the time scale of the pressure perturbation .

The reason for the gravity wave's long lifetime was then investigated by examining the atmospheric structure along the wave path. It was found that a good ducting structure existed as explained by Lindzen and Tung (1976). A statically stable layer was present in the lower troposphere (generally 4 to 5 km thick) which was capped above by a conditionally unstable layer. The capping layer contained the critical level as required by theory. It was also noted that the wave was bounded to the north by frontal zones that disrupted the duct and lead to its demise by dispersion.

The evidence presented shows a remarkable "steady state" in the pressure and precipitation fields associated with the wave as it propagated a great distance across the southeastern United States. This is not surprising considering the ducting theory described earlier. Lindzen and Tung (1976) state that the duct structure controls only the wave's phase speed; wavelength and amplitude are determined by the initial forcing.

To investigate this point further, statistical methods were employed to determine whether any correlation is evident between surface pressure perturbation magnitude and the ducting structure. If there is a relationship, it might be possible to develop a prediction equation for pressure falls to be anticipated with a gravity wave passage. Forecasters, using available sounding data, would then be able to forecast parameters closely associated with pressure perturbations (e.g. wind gusts) more accurately once such a wave has formed.

Four variables were chosen to represent the atmospheric ducting structure: (1) Brunt-Vaisala frequency in the stable layer, (2) thickness of the duct, (3) critical level wind speed; (4) minimum Richardson number in the capping unstable layer. Results of the linear regression (correlation matrix) are shown in table 6.1.

The only significant correlation is that between wave amplitude and static stability (A with B, 0.30). Even this suggests that only about 9% of the variability of perturbation magnitude is due to static stability in the duct. The analysis of variance results, however, show an R^2 value of .4984. This indicates that 50% of the variance in pressure perturbation is explained by the independent variables. Furthermore, the test of the composite hypothesis that all four regression coefficients are zero (i.e. no relationship to the dependent variable) is not significant, that is $F=1.24$ compared to $F(.01,4,5) = 11.39$.

CORRELATION MATRIX

	A	B	C	D	E
A	1.00	0.30	-.01	-.10	-.06
B	0.30	1.00	-.90	-.55	0.17
C	-.01	-.90	1.00	0.53	-.11
D	-.10	-.55	0.53	1.00	0.03
E	-.06	0.17	-.11	0.03	1.00

Table 6.1 Correlation Matrix. A is the surface pressure amplitude, B the Brunt-Vaisala frequency, C the duct thickness, D wind speed at the critical level and E is the minimum Richardson number.

These results seem to substantiate the conclusions of other research that the duct does not control wave characteristics other than the phase speed. Forecasters will instead have to "nowcast", that is rely on persistence. The forecast would be to expect similar weather at their location as was experienced by stations upstream during wave passage. This, of course, would be tempered by any obvious signs of changing conditions. Finally, it was statistically shown that the structure of the duct did not correlate with the observed pressure perturbation magnitude at the ground. This supports the theory that the duct determines only the phase speed; the wavelength and amplitude are determined by the forcing mechanism.

When the general synoptic pattern described by Uccellini and Koch (1986) is seen to develop between the upper level trough and ridge axis forecasters must be alert to the possibility of large amplitude mesoscale gravity waves. Soundings must then be carefully examined for indications of an existing ducting structure, and surface pressure falls monitored. With a duct maintaining the wave structure, associated weather conditions (winds and precipitation being of greatest concern) can be expected to accompany the wave as it propagates over a large horizontal area.

Based on the results of this research, the major conclusions are:

(1) The gravity wave originated over the northwestern Gulf of Mexico, south of Louisiana at about 0200 UTC 6 February 1986.

(2) The most likely physical mechanism responsible for wave initiation was the explosive growth of deep convection.

(3) The wave then travelled northeastwards; reaching the North Carolina coast by 0100 UTC 7 February 1986. This longevity and large horizontal distance covered was due to an atmospheric structure conducive to ducting along the wave path. The wave was bounded to the north by a frontal system. This feature disrupted the duct and led to the gravity wave's dispersion.

(4) Observed propagation velocity of the wave was determined solely by the duct structure.

(5) Amplitudes of maximum pressure perturbations associated with the waves pressure minima are most likely determined by the initial forcing. There was no significant statistical correlation between pressure perturbation and the duct structure. Based on this finding, operational meteorologists would be best served by using persistence when forecasting weather elements expected with wave passage.

6. REFERENCES

- Atkinson, B.W., 1981: Mesoscale Atmospheric Circulations. Academic Press., pp 283-309.
- Balachandran, N.K., 1980: Gravity Waves from Thunderstorms. *Mon. Wea. Rev.*, **108**, 804-816.
- Barnes, S. L., 1964: A Technique for maximizing details in numerical weather map analysis. *J. Appl. Meteor.*, **3**, 396-409.
- , 1973: Mesoscale objective map analysis using weighted time series observations. NOAA Technical Memorandum ERL NSSL-62, Norman, Ok, 60pp.
- , 1985: Omega diagnostics as a supplement to LFM/MOS guidance in weakly forced convective situations. *Mon. Wea. Rev.*, **113**, 2122-2141.
- Bluestein, H.B., 1986: Fronts and Jet Streaks: A theoretical perspective. Mesoscale Meteorology and Forecasting. American Meteorological Society, 793 pp.
- Booker, J. R. and F.P. Bretherton, 1967: The critical layer for internal gravity waves in a shear flow. *J. Fluid Mech.*, **27**, 513-559.
- Bosart, L. F. and A. Seimon, 1988: A case study of an unusually intense gravity wave. *Mon. Wea. Rev.*, **116**, 1857-1886.
- Brunk, I.W., 1949: The pressure pulsation of April 11, 1944. *J. Meteor.*, **6**, 395-401.
- Byers, H.R., 1974: General Meteorology. McGraw-Hill, Inc., New York, 236 pp.
- DeMaria, M., J.M. Davis, and D.M. Wojtak, 1989: Observations of mesoscale wave disturbances during the Genesis of Atlantic Lows Experiment. *Mon. Wea. Rev.*, **117**, 826-842.

- Dirks, R. A., J.P. Kuettner and J.A. Moore, 1988: Genesis of Atlantic Lows Experiment (GALE): An overview. *Bull. Amer. Meteor. Soc.*, **69**, 148-160.
- Erickson, C.O., and L.F. Whitney, Jr., 1973: Gravity waves following severe thunderstorms. *Mon. Wea. Rev.*, **101**, 708-711.
- Gear, J. A., and R. Grimshaw, 1983: A second-order theory for solitary waves in shallow fluid. *Phys. Fluid*, **26**, 14-29.
- Gedzelman, S.D., 1983: Short-period atmospheric gravity waves: A study of their statistical properties and source mechanisms. *Mon. Wea. Rev.*, **111**, 1293-1299.
- , and R.A. Rilling, 1978: Short-period atmospheric gravity waves: A study of their dynamic and synoptic features. *Mon. Wea. Rev.*, **106**, 196-210.
- Gossard, E.E., and W. Munk, 1954: On gravity waves in the Atmosphere. *J. of Meteor.*, **11**, 259-269.
- , and W.H. Hooke, 1975: Waves in the Atmosphere. Developments in atmospheric science, II. Elsevier Scientific Publishing Co., Amsterdam, 456 pp.
- Hoskins, B.J., I. Draghici, and H.C. Davies, 1978: A new look at the omega -equation. *Quart. J. Roy. Meteor. Soc.*, **104**, 31-38.
- Hooke, W.H., 1984: Gravity Waves. AMS intensive course on mesoscale Meteorology and Forecasting, AMS, Boston, Mass. 345 pp.
- Kaplan, M.L., and D.A. Paine, 1977: The observed divergence of the horizontal velocity field and pressure gradient force at the mesoscale: Its implications for the parameterization of three-dimensional momentum transport in synoptic-scale numerical models. *Beitr. Phys. Atmos.*, **50**, 321-330.
- Koch, S.E., 1979: Mesoscale gravity waves as a possible trigger of severe convection along a dryline. Ph.D. Thesis. University of Oklahoma, 195 pp.

- Kreitzberg, C.W., and T.J. Mercer, 1986: Genesis of Atlantic Lows Experiment (GALE) Field Program Summary. Drexel University, Philadelphia, Pa., 217 pp.
- Lin, Y.-L., and R.C. Goff, 1988: A study of a mesoscale solitary wave in the atmosphere originating near a region of deep convection. *J. Atmos. Sci.*, **45**, 194-204.
- Lindzen, R.S., 1974: Wave-CISK in the tropics. *J. Atmos. Sci.*, **31**, 156-179
- , and K.-K. Tung, 1976: Banded convective activity and ducted gravity waves. *Mon. Wea. Rev.*, **104**, 1602-1617.
- Moore, J. T. and P. D. Blakley, 1988: The role of frontogenetical forcing and conditional instability in the midwest snowstorm of 30-31 January 1982. *Mon. Wea. Rev.*, **116**, 2155-2171.
- O'Brien, J.J., 1970: Alternative solutions to the classical vertical velocity problem. *J. Appl. Meteor.*, **9**, 197-203.
- Pencik, M.J., and J.A. Young, 1984: Mechanics of a strong sub-synoptic gravity wave deduced from satellite and surface observations. *J. Atmos. Sci.*, **41**, 1850-1862.
- Raymond, D.J., 1975: A model for predicting the movement of continuously propagating convective storms. *J. Atmos. Sci.*, **32**, 1308-1317.
- Rawlings, J.O., 1988: Applied Regression Analysis: a research tool. Wadsworth and Brooks/ Cole Advanced books and Software, 553 pp.
- Shapiro, R., 1975: Linear Filtering. *Math. Comp.*, **29**, 1094-1097.
- Smith, R.B., and Y.-L. Lin, 1982: The addition of heat to a stratified airstream with application to the dynamics of orographic rain. *Quart. J. Roy. Meteor. Soc.*, **108**, 353-378.

Tepper, M., 1950: A proposed mechanism of squall lines: The pressure jump line. *J. Meteor.*, **7**, 21-29.

Uccellini, L.W., 1975: A case study of apparent gravity wave initiation of severe convective storms. *Mon. Wea. Rev.*, **103**, 497-513.

-----, and S.E. Koch, 1986: The synoptic setting and possible energy sources for mesoscale wave disturbances. *Mon. Wea. Rev.*, **115**, 721-729.

Van Tuyl, A.H., and J.A. Young, 1982: Numerical simulation of nonlinear jet streak adjustment. *Mon. Wea. Rev.*, **110**, 2038-2054.

Wojtak, D.M., 1987: Observation of gravity waves during the Genesis of Atlantic Lows Experiment. M.S. Thesis, North Carolina State University, 75 pp.

Appendix - Objective Analysis Scheme and Numerical Computations

The divergence and vorticity patterns were obtained from objectively analyzed winds at the operational radiosonde network in the south central United States and northern Mexico.

If Q represents any meteorological variable, calculations of grid-point values are obtained by (Barnes, 1964 and 1973):

$$\bar{Q} = \frac{\sum_{i=1}^N w_i Q_i}{\sum_{i=1}^N w_i}$$

The interpolated grid-point value is the weighted mean (\bar{Q}) of observations surrounding the point. N is the total number of stations influencing a given grid point, w_i is the observation weight, and Q_i is the observed value. The observation weights (w_i) are inverse-distance (d) dependent and are defined by: $w_i = \exp(-d^2/4k_0)$. Here, k_0 is the "weight parameter" which controls the rate at which the weight value decreases outward from the point of interpolation. Hence, k_0 determines the degree of smoothing of the data field: if k_0 is small, there is little smoothing; if k_0 is large, there is greater smoothing.

The appropriate choice of k_0 can be determined by selecting the amplitude suppression (response function) of the minimally resolvable wavelength, the latter being twice the average station spacing. The station spacing of the operational radiosonde network in the area of interest is ~ 350 km. If the minimally resolvable waves are suppressed to about 16% of their initial amplitude, the two-pass Barnes theory suggests a weight parameter of about 99,000 km². To obtain this value of k_0 a convergence parameter $\gamma = 0.3$ is used to reduce the weight parameter on the second pass. The amplitude response adopted in this study is consistent with those chosen in other recent applications of the Barnes scheme (Barnes, 1985, 15%; Moore and Blakely, 1988, 21%).

All finite difference calculations were standard second-order centered differences. Objectively interpolated values of wind components were obtained over a 15×19 grid centered over east-central Texas (32° N, 96° W). The grid spacing at the mean latitude of the grid (32° N) is about one-third the station spacing (~ 130 km).

To minimize analysis and computation errors around the edges of the grid, the analysis network included all stations within a box bounded by 40° N , 80° E, 20° S and 115° W latitude - longitude coordinates.